

Dynamical Regge Calculus as Lattice Quantum Gravity

HIROYUKI HAGURA*

*Radiation Science Center,
High Energy Accelerator Research Organization (KEK),
Oho 1-1 Tsukuba-shi Ibaraki 305-0801, Japan*

Abstract

We propose a hybrid model of simplicial quantum gravity by performing at once dynamical triangulations and Regge calculus. A motive for the hybridization is to attempt a dynamical description of topology-changing processes of Euclidean spacetime. In addition, lattice diffeomorphisms as invariance of the simplicial geometry are generated by certain elementary moves in the model. We attempt also a lattice-theoretic derivation of the black hole entropy using the symmetry. Furthermore, numerical simulations of 3D pure gravity are carried out, exhibiting a large hysteresis between two phases. We also measure geometric properties of Euclidean ‘time slice’ based on a geodesic distance, resulting in a fractal structure in the strong-coupling phase. Our hybrid model not only reproduces numerical results consistent with those of dynamical triangulations and Regge calculus, but also opens a possibility of studying quantum black hole physics on the lattice.

*e-mail: hiroyuki.hagura@kek.jp

1 Introduction

One of the most difficult problems in modern physics is the construction of a consistent theory of quantum gravity, whereas Einstein’s theory of classical gravity has been very successful in explaining the large scale structure of spacetime [1]. Many programs to formulate the full quantum theory of gravity are under active research [2, 3, 4]. Since none of them are decisive at present, it is still an open problem to understand what is quantum spacetime at microscopic scales.

In this article we explore a possibility that dynamical Regge calculus [5, 6], which is a hybrid lattice model of dynamical triangulations [7, 8] and quantum Regge calculus [9], gives a possible candidate for a constructive definition of quantum gravity. Although traditional approaches, namely, Regge calculus and dynamical triangulations, have been well studied for a long time as lattice field theories of gravity, they are not satisfactory in several respects. A necessary enlargement of physical degrees of freedom in lattice gravity strongly motivates our study on the hybridization. Actually, the enlargement enables us to define exact “diffeomorphism-invariance” on the lattice at least classically [5].

We will also apply the symmetry to a lattice-theoretic derivation [6] of the Bekenstein-Hawking entropy of a black hole. By the end of 1970’s it was generally accepted that a black hole has the huge entropy \mathcal{S}_{BH} proportional to its horizon area A [17, 18]:

$$\mathcal{S}_{\text{BH}} = \frac{1}{4} k_{\text{B}} \frac{c^3 A}{\hbar G} , \quad (1)$$

where k_{B} is Boltzmann’s constant, c the speed of light and G Newton’s constant¹. Nowadays, it is generally believed that if one sticks to usual theories of gravity (e.g. Einstein’s gravity and dilaton type gravity coupled to normal matter fields), eq. (1) is widely valid [22]. Theoretical explanation of the origin of the huge entropy (1) is considered to be a necessary ingredient for any consistent theory of quantum gravity [20].

Another motive for studying the hybrid model is making an attempt at describing topology-changing processes of Euclidean spacetime in a dynamical way. In a continuum approach Hawking calculated semiclassically the contribution of gravitational instantons to topology-changing processes of four-dimensional Euclidean spacetime manifolds [53] and discussed the processes in connection with Regge calculus; the resultant spacetime that is highly curved and has all possible topologies is called the *spacetime foam*. Such a complicated spacetime is expected to appear in the strong-coupling region of quantum gravity [52], especially inside black holes and in the very early universe. Thus, a question naturally arises: How can we describe the spacetime foam in lattice quantum gravity? It will be shown that the topology-changing processes can in principle occur via degenerate simplicial configurations in our hybrid model.

Regge’s lattice formulation of general relativity [30] has been applied to quantum gravity in two different manners, that is, quantum Regge calculus and dynamical triangulations, as mentioned above. In the former, all link-lengths in a fixed pattern of triangulation (a fixed connectivity of vertices) play the role of dynamical variables. Accordingly, the integration of the link-lengths with a proper functional

¹We write down explicitly all the constants in eq. (1) in order to show how large the black hole entropy is. Indeed, for a black hole of horizon area $A = 1 \text{ cm}^2$, one obtains a huge value $\mathcal{S}_{\text{BH}}/k_{\text{B}} \sim 10^{65}$.

measure is assumed to give a constructive definition of the path integral for the gravitational field $g_{\mu\nu}$. In the latter, in contrast, all patterns of triangulations are regarded as dynamical, while all the link-lengths are fixed to a single lattice spacing a . In this case, the sum over all the possible triangulations is expected to give another constructive definition of the path integral for the gravitational field.

Both lattice models of gravity have merits and demerits; the weakest point common to both of them is the lack of the gauge symmetry that corresponds to ‘reparametrization-invariance’ on the lattice. Actually, one must first give a precise definition of the ‘reparametrization-invariance’ on the lattice in order to construct a ‘gauge-invariant’ measure. We call the symmetry *lattice diffeomorphism-invariance*. Physically, the invariance should be the lattice counterpart of the principle of general covariance. An intention of this article is to discuss the lattice symmetry even on the finite lattice by covering as large degrees of freedom as possible in the space of Riemannian geometries. Thus, one would conjecture that such an enlargement of degrees should be realized by performing *at once* the link-integration arising from quantum Regge calculus and the triangulation-sum arising from dynamical triangulations.

The plan of this article is as follows. In section 2 we give a short review of quantum Regge calculus and dynamical triangulations, making a brief comparison between them. How each formulation regularizes the space of Riemannian geometries is the central issue there. Section 3 deals with the definition of the hybrid model, that is, dynamical Regge calculus, and discuss its fundamental properties. It will also be discussed that topology-changes of discrete spacetime can occur in principle via degenerate simplicial complexes because the lattice action for the gravitational field remains well-defined and finite even on any degenerate configuration that is *not* a manifold. Section 4 considers the symmetric properties, that is, the lattice diffeomorphism-invariance. We will also attempt a lattice-theoretic derivation of the black hole entropy (1) using the lattice symmetry and give a simple interpretation of it in connection with the spacetime uncertainty principle of string theory [49, 50, 51]. Section 5 is devoted to numerical studies of three-dimensional pure gravity. In particular, a fractal structure based on a geodesic distance [44] is measured in detail. As a result, we will obtain a picture of quantum spacetime, which is similar to that obtained in DT. Furthermore, we will acquire several other numerical results consistent with those of both dynamical triangulations and quantum Regge calculus. In section 6 we will summarize our results and discuss several perspectives of dynamical Regge calculus.

2 Quantum Regge calculus vs. dynamical triangulations

In this section we will make a comparison between the two formulations of lattice gravity. We first explain briefly the idea of the Euclidean path integral approach in the continuum, and then present a basics of Regge calculus. Emphasis is laid on geometric properties on the finite lattice.

2.1 Regge’s formulation

Leaving aside the lattice approaches for a moment, let us look at the Euclidean path-integral approach in the continuum [24]. The basic object of the approach is the functional integral for the

metric field $g_{\mu\nu}$ of Euclidean signature $++\cdots+$:

$$Z_{\text{cont}} = \int \frac{\mathcal{D}g}{\text{Vol}(\text{Diff}_M)} \exp\left(-S_{\text{EH}}[g]\right) , \quad (2)$$

where $S_{\text{EH}}[g]$ is the Einstein-Hilbert action on a d -dimensional Euclidean spacetime M :

$$S_{\text{EH}}[g] = -\frac{1}{16\pi G} \int_M d^d x \sqrt{g} (R - 2\Lambda) . \quad (3)$$

Here Λ is the cosmological constant, and units are such that $c = \hbar = 1$. For simplicity, we assume M to be a compact, closed manifold of a fixed topology. The integration (2) is taken over the space of the metric field $g_{\mu\nu}$ with an appropriate functional measure $\mathcal{D}g$.

The groundwork for the path integral approach was laid by De Witt [27], and subsequently detailed prescriptions were developed by Gibbons, Hawking and Perry [28]. Although this approach has several difficulties and unsolved problems, a number of highly suggestive results have been obtained. Presumably, the dramatic successes of this approach are that, as mentioned in introduction, the foam picture of spacetime can be established semiclassically by calculating the contribution of the gravitational instantons [53], and that the creation of particles near a Schwarzschild black hole can be related in a direct and simple manner to the properties of the Euclidean Schwarzschild solution [19].

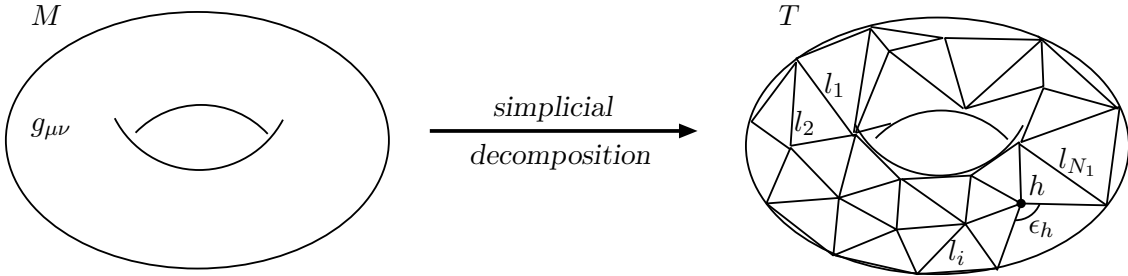


Figure 1: An example of the simplicial decomposition. A smooth manifold M with a metric g is replaced by a simplicial manifold T with a set of link-lengths $\{l_1, l_2, \dots, l_i, \dots, l_{N_1}\}$. ϵ_h is the deficit angle around a hinge (vertex) h , corresponding to the scalar curvature. In two dimensions the volume, A_h , of the hinge h is defined to be 1, while A_h takes non-trivial values in higher dimensions.

Having shortly surveyed the continuum approach, let us now return to our main interest. In Regge's lattice formulation of general relativity [30], the continuum spacetime M is replaced by a discretized space T that consists of a finite number of d -simplices, as shown in Fig. 1. Such a discrete space T is called a d -dimensional *simplicial manifold* or *triangulation* in lattice gravity². First, we give a connectivity of vertices in T , which must satisfy the manifold condition that the space looks locally like a Euclidean space \mathbf{R}^d . Incidentally, the total number, N_k , of k -simplices also is determined ($k = 0, 1, \dots, d$). Next, we give lengths l_1, l_2, \dots, l_{N_1} to all the links (1-simplices) in T . As a result,

²Exactly speaking, the discrete counterpart of a Riemannian manifold $(M, g_{\mu\nu})$ is a *piecewise linear (PL) manifold*, which has a certain metric structure that converges on the Riemannian structure in a continuum limit [16]. In other words, a simplicial manifold equipped with a PL metric structure is assumed to be a (discrete) physical spacetime.

the pair of the connectivity and the set of all the link-lengths $\{l_i\}$ determine the simplicial geometry on the discrete spacetime T .

The above procedure is called the *simplicial decomposition*. An example of the procedure is depicted on Fig. 1, where a two-dimensional torus with a metric $g_{\mu\nu}$ is decomposed to a simplicial torus with the link-lengths $\{l_i\}$ by gluing triangles (2-simplices) along their boundary links (1-simplices). On the simplicial manifold, in general, one can define geometric quantities (differential forms, curvatures, parallel transport, etc.) in a standard way. In particular, the Einstein-Hilbert action (3) is replaced with the *Regge action*, S_{Regge} , on T [30]:

$$S_{\text{Regge}}[l, T] = -\frac{1}{16\pi G} \sum_{h:\text{hinges}} 2A_h \epsilon_h + \Lambda \sum_{\sigma:d\text{-simplices}} V_\sigma, \quad (4)$$

where A_h and V_σ are volumes of a $(d-2)$ -simplex (*hinge*) h and of a d -simplex σ . The dimensionless quantity ϵ_h in the right hand side of (4) is called the deficit angle around the hinge h , which plays the role of the local scalar curvature on T . The symbol l denotes the set of all the lengths $\{l_1, l_2, \dots, l_{N_l}\}$.

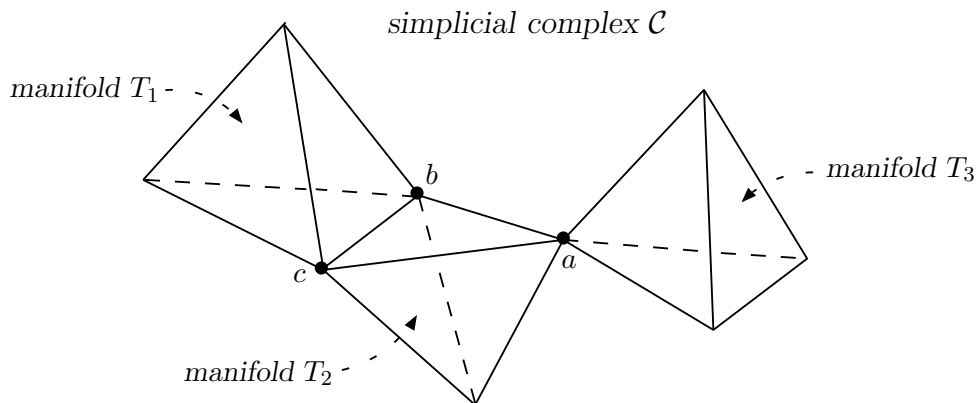


Figure 2: An example of a simplicial complex \mathcal{C} that is not a manifold. The complex \mathcal{C} is a union of three simplicial (sub)manifolds T_i ($i = 1, 2, 3$), and obviously violates the manifold condition at the junction parts, namely, at the vertex a and along the link bc . The Regge action $S_{\text{Regge}}[l, T_i]$ is well-defined and finite on each T_i . Furthermore, the Regge action $S_{\text{Regge}}[l, \mathcal{C}]$ on \mathcal{C} is also defined uniquely as the sum of the actions $S_{\text{Regge}}[l, T_i]$ ($i = 1, 2, 3$).

Interestingly, the Regge action (4) is well-defined even on a degenerate configuration that is *not* a simplicial manifold but a *simplicial complex*. The crucial difference between the simplicial manifold and the simplicial complex is that the former satisfies the manifold condition that the space looks locally like a Euclidean space \mathbf{R}^d , but the latter does *not necessarily*. Fig. 2 shows a two-dimensional simplicial complex \mathcal{C} which is not a manifold of definite dimension; the manifold condition is violated at the junction parts. However, the Regge action $S_{\text{Regge}}[l, \mathcal{C}]$ on \mathcal{C} is uniquely defined as the sum of the actions $S_{\text{Regge}}[l, T_i]$ ($i = 1, 2, 3$) where T_i are simplicial submanifolds of the complex \mathcal{C} . Unlike the case of the continuum action (3), the finiteness of the Regge action (4) even on such a degenerate complex is an essential feature, particularly for describing the topology-change of Euclidean spacetime in later section 3.3.

2.2 Quantum Regge calculus

From now on let us concentrate on the problem of lattice quantization of gravity based on Regge calculus (RC). In quantum RC the discretized equivalent of the integration over the metrics (2) is implemented by *varying the link-lengths on a fixed triangulation*, assuming that patterns of triangulations are not dynamical at all; this is the reason why quantum RC is often called the *fixed triangulation (FT) approach*. Accordingly, the partition function for quantum Regge calculus on a fixed triangulation T is given by

$$Z_{\text{RC}}[T] = \int d\mu_T[l] \exp\left(-S_{\text{Regge}}[l, T]\right), \quad (5)$$

where $d\mu_T[l]$ is a link-integration measure defined on T , including constraints imposed by the (higher-dimensional analogs of) triangle inequalities. Each length l_i is integrated over a range $l_{\min} < l_i < l_{\max}$. In eq. (5) we explicitly write down the ‘subscript’ T of the measure $d\mu_T[l]$ and the ‘variable’ T for the partition function $Z_{\text{RC}}[T]$ in order to make it clear that they are defined on the triangulation T . This notation is useful for our formulation.

The FT approach (5) has been actively applied to quantization of gravity [9, 10], and actually has many appealing aspects. However, this approach has some subtle issues. One of them is how to define the discretized measure $d\mu_T[l]$ that corresponds to the continuum measure $\mathcal{D}g$ in eq. (2) over the so-called superspace [31] of the Riemannian metrics on M . In fact, one has to gauge away the diffeomorphism group Diff_M that is the gauge freedom of general relativity. In the continuum a possibility is to start from the supermetric formulation [32] that defines a gauge-invariant measure over the superspace and then to gauge away Diff_M by using one’s favorite gauge.

Here one would ask a simple question: what is the lattice counterpart of the diffeomorphism group Diff_M ? In what follows, we explain the notion of “diffeomorphism” on the lattice, which has been used at two different levels [34]. One definition of the symmetry, which is often adopted by those studying Regge calculus in classical relativity, is called “invariance of the geometry” in which transformations of link-lengths leave the *geometry* invariant. A proper implementation of it is to require that all local curvatures (and hence all deficit angles) should be unchanged under the transformations. But this requirement is too strong to satisfy in the FT approach³ [12].

Another definition, favored by those wishing to use results from lattice gauge theories, is referred to as “invariance of the action” in which transformations of link-lengths leave the *action* invariant. It is possible even in RC to imagine that changes in the link-lengths which could increase deficit angles in one region and compensatingly decrease them in another would produce no overall change in the Regge action (4). In quantum RC, however, the symmetry in this sense holds approximately at most in (almost) flat space [11, 12, 13]; still less it would be possible to find in curved space any exact symmetry that can be interpreted as the lattice diffeomorphism in the FT approach.

The other problem is that there can be generally singular configurations including such simplices that have very short and very long links at the same time, as shown in Fig. 3. Though one usually

³The only exception is flat space where an infinite number of choices of the link-lengths will generally correspond to the same flat geometry even in the case of RC.

deals with this problem by putting upper and lower bounds on the lengths l_i , such configurations are unavoidable to obtain a metric with very high curvature out of the flat metric. It is still unclear whether one can explore regions in the space of metrics where the metric is very singular and fairly different from the typical metric on the reference simplicial space that we have chosen at the beginning. It will cause a large difficulty in studying the strong-coupling region of lattice quantum gravity, where configurations with very high curvatures are expected to emerge frequently.



Figure 3: Singular configurations arising in the FT approach. (a) A singular 2-simplex. (b) A singular 3-simplex.

2.3 Dynamical triangulations

In the dynamical triangulation (DT) approach [7, 8], which is the alternative to the FT one, one assumes that none of the link-lengths in each triangulation are dynamical and all of them can be fixed to a single lattice spacing a . Accordingly, the simplicial manifold T considered in DT consists of equilateral d -simplices. The Regge action (4) on such a equilateral triangulation T becomes the following simple form:

$$S_{\text{DT}}[T] = -\kappa_0 N_0 + \kappa_d N_d , \quad (6)$$

where κ_0 and κ_d are constants related to G , Λ and a . N_0 and N_d stand for the number of 0-simplices and that of d -simplices on T . Instead of the link-lengths, we take *varying connectivity of vertices* as dynamical. Hence, the path integral for DT is defined by the sum over all possible patterns of triangulations that consist of equilateral d -simplices:

$$Z_{\text{DT}} = \sum_{T:\text{triangulations}} \exp\left(-S_{\text{DT}}[T]\right) . \quad (7)$$

Here we fix the topology of all the triangulations T .

In what follows, we make a brief comparison between FT (5) and DT (7) to clarify the differences between them. For any Riemannian manifold non-singular enough to start as the reference at the beginning, one can construct a sequence of simplicial manifolds. We expect that in DT the discrete set of simplicial spaces is regularly distributed in the space of all the Riemannian metrics [33], as shown in Fig. 4 (a). In contrast, simplicial spaces arising in FT are localized in the neighborhood of the smooth metric on the regular lattice that has been chosen at the beginning (see Fig. 4 (b)); such a localization will make the lattice configurations less accessible to the strong-coupling regions that might be far from the reference metric, and further prevent lattice diffeomorphism-invariance from holding. In this respect, DT has the advantage over FT. Moreover, DT has the natural UV cutoff a of the theory.

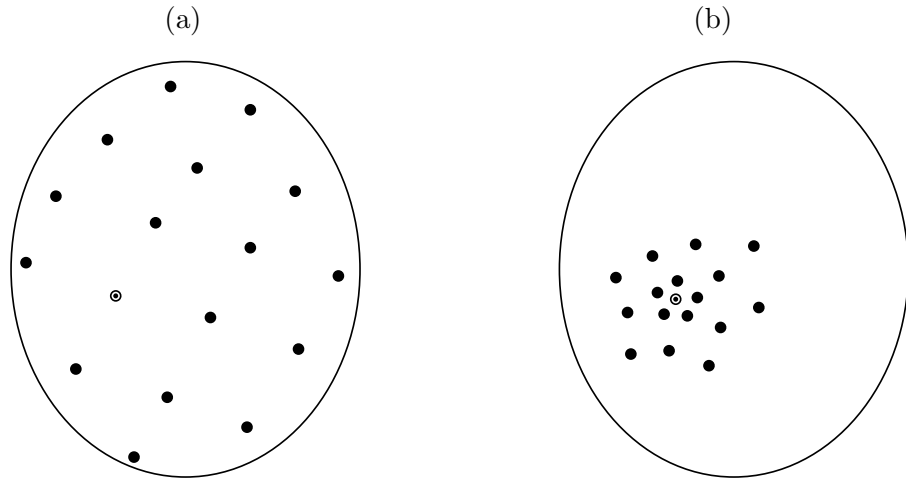


Figure 4: Sketch of the space of all Riemannian metrics. Each point means a simplicial geometry. The circles with dot represent the reference (flat) simplicial space at the beginning. (a) “Regular” distribution arising in the DT approach. (b) “Localized ” distribution around the reference metric arising in the FT approach.

Nevertheless, the DT approach makes some issues more difficult. Actually, we have completely lost diffeomorphism-invariance on the lattice, because one cannot deform smoothly (even approximately) a simplicial lattice into another in this approach. Some argue that in DT the permutation group S_{N_0} acting on N_0 vertices is expected to reproduce the diffeomorphism group acting on a smooth manifold in a continuum limit⁴, although no exact proof has been known yet. One has to check whether diffeomorphism-invariance is recovered in the continuum limit⁵, if it exists. In addition, it is not clear how to define the classical continuum limit of DT, since this approach gives no field equation corresponding to Einstein’s equation. As a consequence, this difficulty makes it fairly intractable to study (quantum) black hole physics in DT.

Given reasonable geometric and symmetric properties, universality in quantum field theory will assure the same results for physical observables in a certain continuum limit, even though the details of UV behaviors of FT and DT are different from each other. This is almost the case with lattice field theories, where physical results are expected to be independent of specific details of the UV cutoff and the specific form of the lattice action as long as theories of interest preserve the underlying symmetries. In the case of lattice gravity, however, such an expectation from universality will not necessarily hold, because the two approaches have different symmetric properties as discussed above. Exactly speaking, it is a drawback to the lattice regularizations of gravity that they lack diffeomorphism-invariance even at the classical level, in contrast to other lattice field theories where gauge symmetries are (classically) exact on the finite lattice. An attempt to overcome the drawback strongly motivates us to study the hybrid model of quantum RC and DT, namely, dynamical Regge calculus.

⁴In the IIB matrix model, which is a candidate for a constructive definition of superstring theory, the same scenario is also discussed [42].

⁵In the case of two-dimensional quantum gravity, however, it has been verified that results obtained in DT [8] coincide with the predictions from CFT [25] and diffeomorphism-invariance is recovered in two dimensions.

3 Dynamical Regge calculus

In this section we first give the definition of our hybrid model as a simultaneous implementation of quantum RC and DT, and then discuss its fundamental properties. We also discuss possible behaviors of the entropy⁶ of the model, which is related directly to the well-definedness of the model. Moreover, we apply the hybrid model to a topology-changing process of Euclidean spacetime on the lattice. Finally, we formulate elementary local moves necessary to carry out numerical simulations.

3.1 Definition of the hybrid model

The partition function, Z_{DRC} , of *dynamical Regge calculus* (DRC) is defined by performing *at once* the link-integration (5) and the triangulation-sum (7):

$$Z_{\text{DRC}} = \sum_{T:\text{triangulations}} \int d\mu_T[l] \exp(-S_{\text{Regge}}[l, T]) = \sum_{T:\text{triangulations}} Z_{\text{RC}}[T] , \quad (8)$$

where each link-length l_i is integrated over the range $l_{\min} < l_i < l_{\max}$. The sum $\sum_{T:\text{triangulations}} \int d\mu_T[l]$ means that any pattern of triangulation (connectivity of vertices) T with various sets of the link-lengths is included so long as it satisfies both the manifold condition and the triangle inequalities (see Fig. 5). The reason for the name of dynamical Regge calculus is that Regge calculus $Z_{\text{RC}}[T]$ on each triangulation T (see eq. (5)) is thought of as if a ‘dynamical variable’ in the partition sum (8).

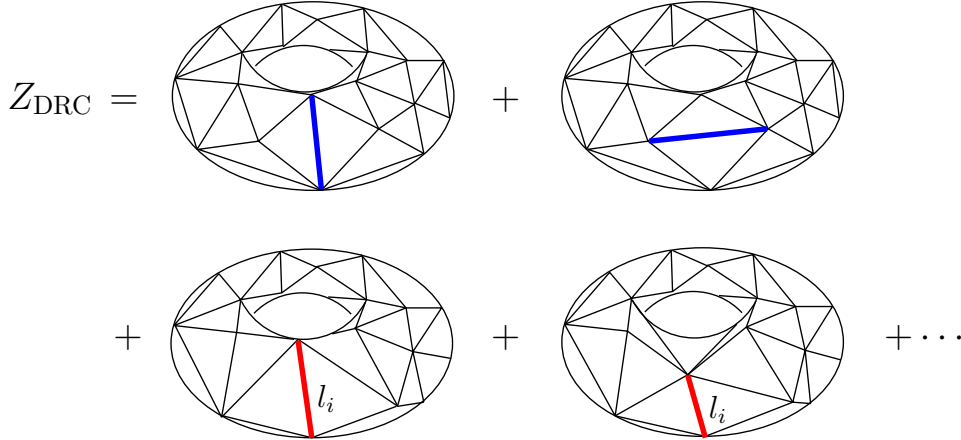


Figure 5: *Lattice configurations appearing in the sum (8). The first two configurations have different patterns of connectivity, arising from the triangulation-sum \sum_T . The next two have the same connectivity but contain different lengths of the i -th link, arising from the link-integration $\int d\mu_T[l]$.*

A few remarks are in order. First, the behavior of the entropy of the hybrid model (8) is essential to its well-definedness as a statistical system. A natural generalization from DT leads to the following definition of the entropy, $W(N_d)$, of the model (8):

$$W(N_d) \equiv \sum_{T:N_d \text{ fixed}} \int d\mu_T[l] , \quad (9)$$

⁶Here the entropy means the total number of possible triangulations in the model and, therefore, it is *not* the black hole entropy. Do not be confused with the same term ‘entropy’.

where the sum $\sum_{T:N_d \text{ fixed}}$ is taken over triangulations with the number of d -simplices N_d fixed. It depends strongly on the behavior of the entropy (9) whether the model (8) is well-defined statistical-mechanically or not. If we set the coupling constant $G = \infty$ for simplicity, the following inequality holds:

$$e^{-S_{\text{Regge}}[l, T]} < e^{-\Lambda l_{\min}^d N_d} , \quad (10)$$

where the minimal length l_{\min} plays the role of the UV cutoff. Thus, for the partition function $\tilde{Z}_{\text{DRC}}(N_d)$ with N_d fixed, one easily obtains the following inequality:

$$\begin{aligned} \tilde{Z}_{\text{DRC}}(N_d) &\equiv \sum_{T:N_d \text{ fixed}} \int d\mu_T[l] \exp(-S_{\text{Regge}}[l, T]) \\ &< W(N_d) e^{-\Lambda l_{\min}^d N_d} . \end{aligned} \quad (11)$$

If an exponential bound for the entropy $W(N_d)$ holds

$$W(N_d) < \text{const.} \times e^{\Lambda_c l_{\min}^d N_d} \quad (\Lambda_c; \text{ a positive constant}) , \quad (12)$$

then DRC (8) is well-defined at least as a statistical system. In this case it is a possibility that one can take a continuum limit by fine-tuning the cosmological constant Λ . However, it is very hard to give any analytic proof for the exponential bound (12) because the integration measure $d\mu_T[l]$ includes the triangle inequalities which are too intractable to calculate analytically. Instead, we will later see a piece of numerical evidence that the bound (12) holds in case that we use the scale-invariant measure $\prod_i dl_i/l_i$.

Second, we comment on the relationship between DT (7) and DRC (8). If one chooses the δ -function measure

$$d\mu_T[l] = \prod_i dl_i \delta(l_i - a) , \quad (13)$$

then DRC (8) becomes the same as DT (7) where all the lengths are fixed to the single lattice spacing a and the triangle inequalities are automatically satisfied. In other words, DT is equivalent to DRC with the δ -function measure (13). As is well known with matrix models [26], such a choice (13) gives a constructive definition of two-dimensional quantum gravity, although the measure (13) breaks explicitly the lattice diffeomorphism-invariance. Although the problem of the lattice symmetry is not dealt with here, we will observe in section 4 that it is a difficult task to construct a ‘diffeomorphism-invariant’ measure on the lattice.

3.2 Hybrid (p, q) moves in DRC

Here we construct local, ergodic moves, i.e., local changes of triangulations, though the action of the moves never changes topology of the simplicial manifold; such elementary moves are a necessary ingredient to carry out numerical studies of DRC (8). The Monte-Carlo method is applicable to DRC[5, 6], as well as it has been so to both quantum RC [11, 13] and DT [8]. Remember that in

DT the so-called (p, q) moves⁷ are used and they are ergodic in the class of triangulations of fixed topology [40]. In what follows, we give an extension of the (p, q) moves to invoke quantum RC in addition to DT according to DRC (8).

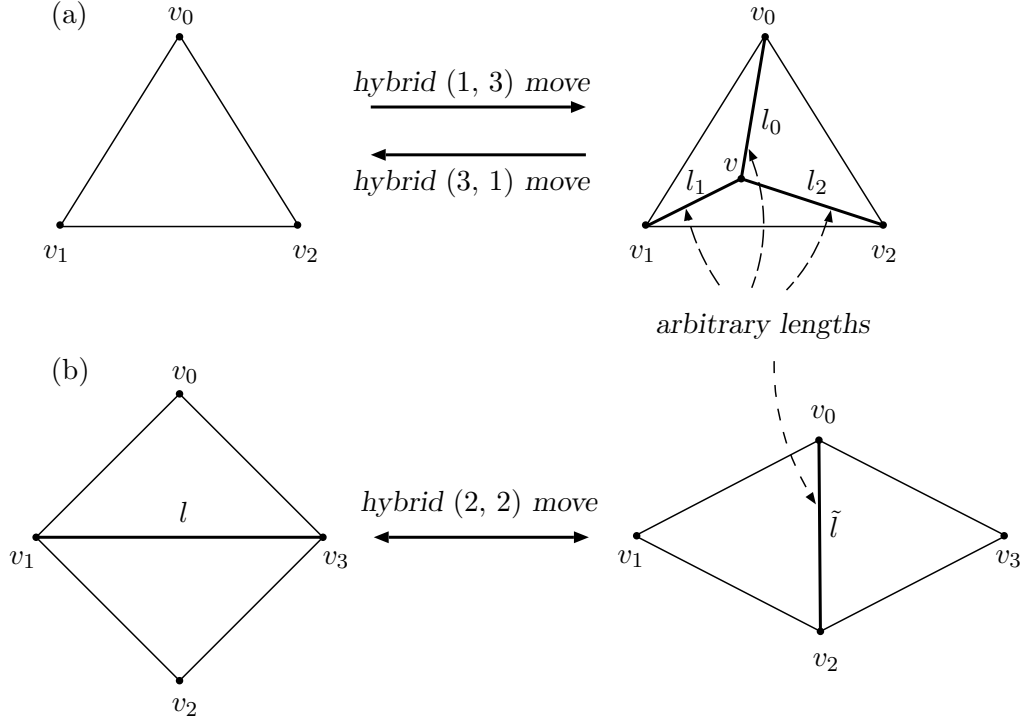


Figure 6: Hybrid (p, q) moves in two dimensions. (a) A hybrid (1, 3) move, where the triangle $v_0v_1v_2$ is divided into three triangles vv_0v_1 , vv_1v_2 and vv_2v_0 . Then, inserted links vv_0 , vv_1 and vv_2 can take arbitrary lengths so long as triangle inequalities hold. Its inverse move, called the hybrid (3, 1) move, is also depicted. (b) A hybrid (2, 2) move acting on two triangles $v_0v_1v_3 + v_1v_2v_3$. After deleting the link v_1v_3 of length l , a new link v_0v_2 of length \tilde{l} is inserted. The length \tilde{l} is also arbitrary unless triangle inequalities are broken.

In Fig. 6, we show an example of the extended moves in two-dimensions; in Fig. 6 (a), a triangle $v_0v_1v_2$ is divided to three new triangles vv_0v_1 , vv_1v_2 and vv_2v_0 by inserting a vertex v and three new links vv_0 , vv_1 , vv_2 . The link-lengths are arbitrary as long as triangle inequalities hold. The deficit angles around the vertices v_0 , v_1 , v_2 and v can change continuously in DRC as well as in quantum RC⁸. The inverse move is defined straightforwardly, as shown in Fig. 6 (a). We call the two moves of Fig. 6 (a) the *hybrid (1, 3) move* and the *hybrid (3, 1) move*. Similarly, one can extend the (2, 2) move of DT to a hybrid one of DRC, as depicted on Fig. 6 (b). The link v_1v_3 of length l shared by two triangles $v_0v_1v_3$ and $v_1v_2v_3$ is flipped to a new link v_0v_2 of length \tilde{l} ; \tilde{l} also is arbitrary unless triangle inequalities are broken, and hence, the deficit angles around the vertices v_0 , v_1 , v_2 and v_3 can take continuous values. We call the extended move in Fig. 6 (b) the *hybrid (2, 2) move*.

⁷In ref. [40], these moves are called the (k, l) moves. To avoid confusion, however, we use here the term of the (p, q) moves instead, since we use the symbol l to denote (a set of) link-lengths.

⁸Indeed, we observe soon later that the link-integration of quantum RC is automatically included in such moves.

It is straightforward to generalize the two-dimensional hybrid (p, q) moves to higher-dimensional ones, where $p + q = d + 2$ ($d = 3, 4$). For example, Fig. 7 shows three-dimensional hybrid (p, q) moves.

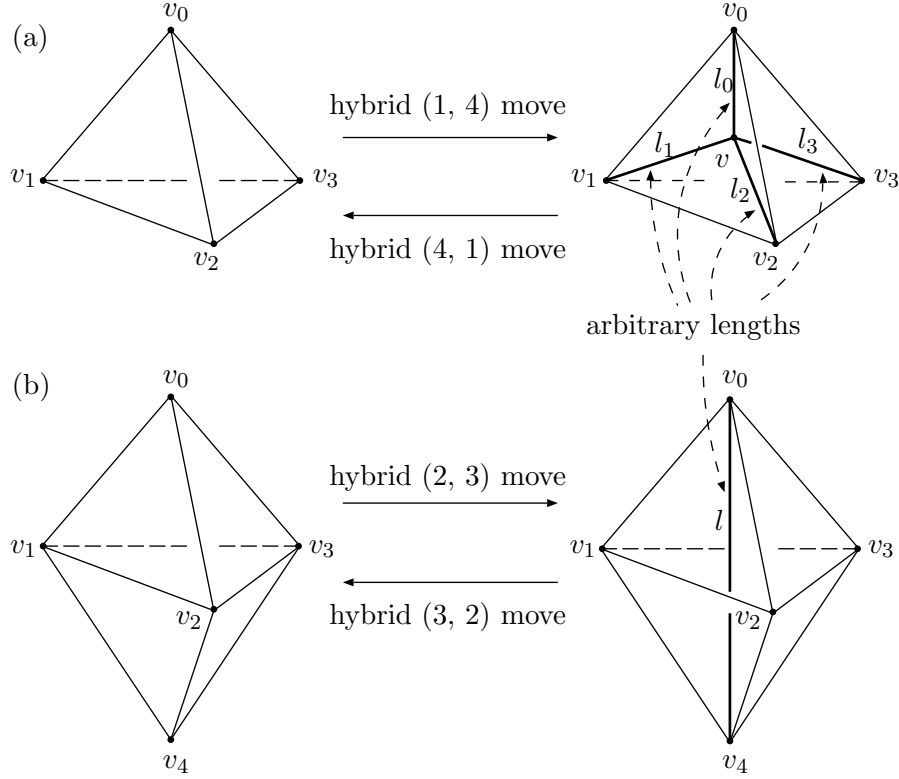


Figure 7: Hybrid (p, q) moves in three dimensions. (a) A hybrid $(1, 4)$ move, where a new vertex v is put into the 3-simplex $vv_0v_1v_2v_3$ and four links vv_0 , vv_1 , vv_2 and vv_3 with arbitrary lengths l_0 , l_1 , l_2 and l_3 are inserted unless triangle inequalities are broken. Its inverse move is also depicted. (b) A hybrid $(2, 3)$ move acting on two 3-simplices $v_0v_1v_2v_3 + v_1v_2v_3v_4$. Instead of the triangle $v_1v_2v_3$, the new link v_0v_4 is inserted. The length l of v_0v_4 is arbitrary so long as triangle inequalities hold. Its inverse moves, called the hybrid $(3, 2)$ move, is also shown.

The hybrid (p, q) moves described above are ergodic in the same sense that the usual (p, q) moves are ergodic in DT. Moreover, we explain how below the hybrid moves implement not only DT but also quantum RC, as shown in Fig. 8. A link-integration will be done by successive applications of the hybrid moves as follows:

- M1) On a two-dimensional simplicial lattice we pick up a link uv of length l_i (see Fig 8 (a)). Then, we apply a hybrid $(2, 2)$ move to the link uv , and a new link ab is created (see Fig 8 (b)).
- M2) Another hybrid $(2, 2)$ move is applied to the link ab , getting back to the same connectivity as the initial configuration (see Fig 8 (c)). The only difference between the initial and final configurations is that the length l_i of the link uv is replaced with the different one l_f .

Through the process M1) and M2), the length of the link uv has changed from the initial l_i to the final one l_f according to the proper Boltzmann weight. Hence, this is a typical example of realization of quantum RC only by the combinations of the hybrid moves.

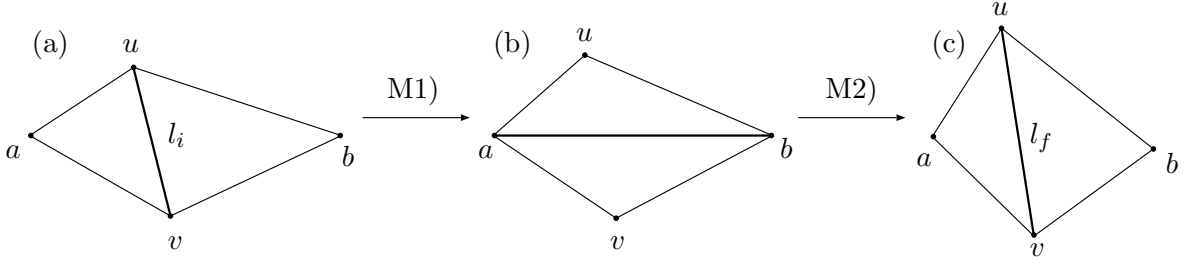


Figure 8: An example of realization of a link-integration by successive applications of the hybrid (p, q) moves in two dimensions. Through the first hybrid $(2, 2)$ move M1), the link uv of length l_i is flipped to a link ab . The next hybrid $(2, 2)$ move M2) changes the link ab back to the link uv of length l_f . As a result, this process realizes a link-integration of quantum RC only by the hybrid moves.

In general, one guesses that in higher dimensions similar combinations of the hybrid moves can incorporate the link-integrations of RC into DRC. This is really the case with our hybrid model. In addition to the link-integration discussed above, the hybrid (p, q) moves are ergodic in the sense that all the patterns of triangulations can be generated by the hybrid moves owing to the ergodic property of the usual (p, q) moves in DT [40]. As a consequence, these properties completes the ergodicity of the hybrid (p, q) moves in DRC.

3.3 Description of topology change in DRC

As an application of the hybrid model, we attempt to describe topology-changing processes of Euclidean spacetime on the lattice. For the purpose, we need to extend our model (8) in order to deal with degenerate configurations that appear in the topology change, as will be discussed below.

Over forty years ago, Wheeler pointed out [52] that the Einstein-Hilbert action (3) allows large fluctuations of the metric and even of the topology of spacetime manifolds on scales of order of the Planck length. This is due to the fact that the action for the gravitational field (3) is not scale invariant, unlike that for the Yang-Mills fields. Hence, a large fluctuation of the metric over a short length scale does not have a very large value of the action and so is not highly damped in the path integral (2). The resultant quantum spacetime with the large fluctuations of both the metric and the topology is called the *spacetime foam*. Subsequently, Hawking calculated semiclassically the path integral for the spacetime foam by summing up “gravitational instantons⁹” with various Euler numbers χ in four dimensions [53]. Physically, the “gravitational instantons” describe the topology-change of Euclidean spacetime. Furthermore, Hawking discussed a dynamical realization of such a topology-changing process by using quantum Regge calculus; a metric can change topology without increasing the lattice action by more than an arbitrary small amount [53]. In what follows, we explain the close relation between Hawking’s idea and our hybrid model.

We first define the partition function, Z_{EDRC} , of the extended hybrid model:

$$Z_{\text{EDRC}} = \sum_{\mathcal{C}:\text{complexes}} \int d\mu_{\mathcal{C}}[l] \exp\left(-S_{\text{Regge}}[l, \mathcal{C}]\right) = \sum_{\mathcal{C}:\text{complexes}} Z_{\text{RC}}[\mathcal{C}] , \quad (14)$$

⁹For a detailed explanation of the gravitational instantons, see ref. [54].

where the sum $\sum_{C:\text{complexes}} \int d\mu_C[l]$ admits degenerate simplicial complexes (see Fig. 2) in addition to simplicial manifolds. Furthermore, manifolds (or complexes) of various topologies are contained in the extended sum (14) for a dynamical description of topology-changing processes.

Now we discuss a simple example of Fig. 9 to illustrate a process of changing continuously from the topology of one simplicial manifold to the topology of another. Consider a simplicial manifold S^2 with a ‘waist’ triangle abc (Fig. 9 (a)). The three links ab, ac and bc of the ‘waist’ has lengths l_{ab}, l_{ac} and l_{bc} , respectively and satisfy the triangle inequality $l_{ab} < l_{ac} + l_{bc}$. The manifold has Euler number $\chi = 2$, where χ is defined on the lattice as

$$\chi = N_0 - N_1 + N_2 .$$

Here N_k stands for the number of k -simplices ($k = 0, 1, 2$). Once an equality $l_{ab} = l_{ac} + l_{bc}$ holds by varying the link-lengths, the triangle abc will collapse to a singular link along which the manifold condition does not hold any longer (Fig. 9 (b)). In general, if some of the (sub)simplices collapse to lower dimensions, a simplicial complex will not remain a manifold but become a degenerate configuration; this is the case with the simplicial complex shown in Fig. 9 (b).

Subsequently, we delete four 2-simplices adc, bdc, bec and eac around c , while combining the two links ac and cb into a new link ab . Then, c is deleted. Moreover, a separation of the new link ab (dashed) from the old ab (solid) will lead to other degenerate complex shown in Fig. 9 (c). The shaded part is an empty region on which no (sub)simplex resides. Although the simplicial complex is no longer a manifold, the Regge action (4) remains well-defined and finite even on such degenerate configurations shown in Figs. 9 (b) and (c). The process from (b) to (c) is beyond the link-integration (of RC) and the usual (p, q) moves (of DT) [40]; in general, such a process should be called a *surgey* acting on the simplicial complex.

Next step is to apply the hybrid (p, q) moves around a and b . As a result, we can obtain a simplicial complex as shown in Fig. 9 (d), in which coordination numbers of a and b are three. However, the complex has apparently Euler number $\chi = 2$, though it is *not* a manifold of definite dimension and topology.

Finally, we “blow up” the degenerate simplicial complex to obtain a new simplicial manifold. We delete six 2-simplices around a , that is, $aa_1a_2, aa_2a_3, aa_3a_1, aa'_1a'_2, aa'_2a'_3$ and $aa'_3a'_1$ in Fig. 9 (d). Then a is deleted, while we identify a_i with a'_i ($i = 1, 2, 3$) pairwise. Similarly, we delete six 2-simplices around b , and identify b_i with b'_i ($i = 1, 2, 3$). As a consequence of the “blowing-up” surgery, the degenerate complex of Fig. 9 (d) has changed to a simplicial manifold T^2 of Fig. 9 (e).

In this way, one can pass continuously from one metric topology to another with the Regge action remaining finite. Indeed, one could deform the topology of the simplicial manifold only by the action of such local moves within the framework of extended DRC (14). However, we meet with a difficulty in finding a minimal set of elementary moves that are local and ergodic. In other words, we do not know which set of moves can generate all the configurations in the class of simplicial complexes of various topologies. This is due to the surgery operations, such as the process from Fig. 9 (b) to (c) or the process from Fig. 9 (d) to (e). Thereby, it is very hard for us to study numerically the extended model (14).

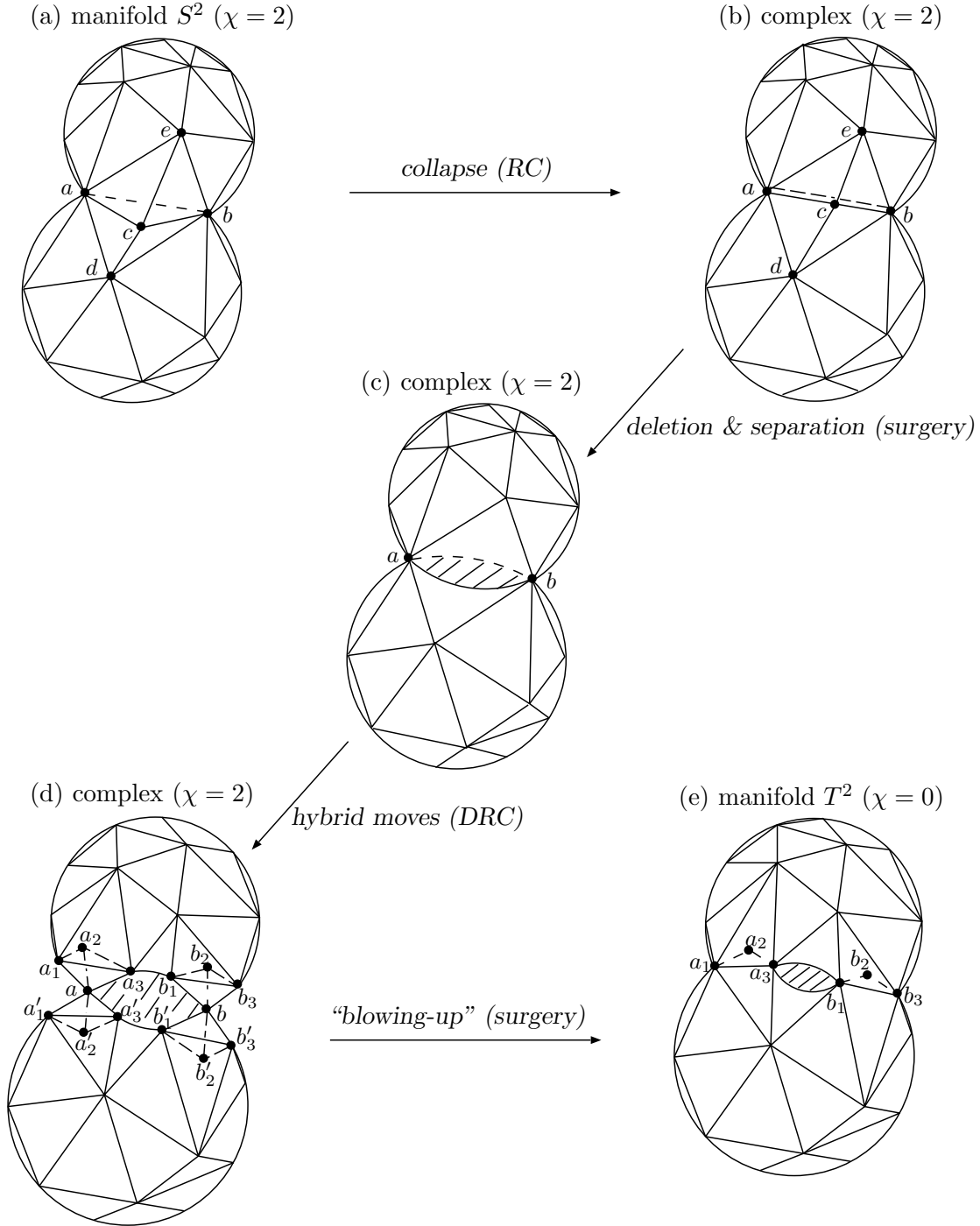


Figure 9: An example of topology-changing process via degenerate complexes in extended DRC (14). (a) A simplicial manifold S^2 of $\chi = 2$ has a ‘waist’ triangle abc . (b) If three links of abc satisfy $l_{ab} = l_{ac} + l_{bc}$, then abc collapses to a (singular) link. The configuration is now not a manifold but a degenerate complex. (c) The four 2-simplices sharing the 0-simplex c are deleted. But we leave the two 1-simplices ac and bc and combine them into another 1-simplex ab (solid curve), and then delete c . The dashed curve is the old ab . The shaded region between the two ab becomes empty. (d) By acting the hybrid (p, q) moves around a and b , the two vertices will have coordination number three. The complex still has $\chi = 2$. (e) We delete six 2-simplices around a and further six 2-simplices around b . Then, the 0-simplices a_i and a'_i ($i = 1, 2, 3$) are identified and, similarly, b_i and b'_i ($i = 1, 2, 3$) are done. The complex changes to a simplicial manifold T^2 of $\chi = 0$ by the “blowing-up” surgery.

4 Lattice diffeomorphisms in DRC

When a Riemannian manifold (M, g) is given, there is arbitrariness in choosing coordinate-systems that cover a manifold M . The arbitrariness is necessary to represent the principle of general covariance in general relativity. Similarly, in the case of discrete gravity, the freedom would be reflected as the existence of the infinite number of triangulations that correspond to the same Riemannian geometry; they should be transformed into each other by “lattice diffeomorphisms” defined on the simplicial manifold. An important issue in regularized theories of quantum gravity is the nature of symmetric properties. Although active discussions on the issue have been given, systematic formulations of the lattice diffeomorphisms have not yet been established. Actually, in the FT approach diffeomorphism-invariance is approximately realized as the appearance of gauge zero modes only on (almost) flat backgrounds [12, 13, 14]; by the method of lattice weak-field expansion, the zero modes and the corresponding eigenvectors identified with infinitesimal local coordinate transformations in a continuum limit. But invariance properties on curved backgrounds are beyond the scope of the weak-field expansion.

In this section we will observe that the Regge action (4) on arbitrary curved backgrounds is exactly invariant under certain hybrid (p, q) moves in (extended) DRC and further that such moves are interpreted as the lattice diffeomorphisms in a natural way.

4.1 Invariance (p, q) moves on the simplicial complex

As an illustrative example, let us construct such a hybrid $(2, 2)$ move that keeps the Regge action (4) exactly invariant. We zoom up some 2-simplices around a hinge (vertex) h on a triangulated surface. We put them on a flat \mathbf{R}^2 plane to make explicitly visible the deficit angle ϵ_h around h , as depicted on

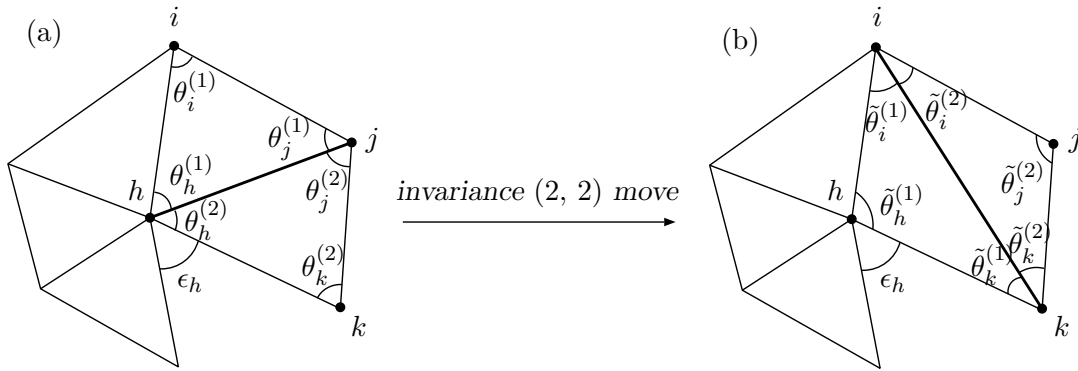


Figure 10: *Example of the invariance $(2, 2)$ move which keeps the simplicial geometry and the Regge action (4) invariant. (a) Some triangles sharing the hinge h are put on a flat \mathbf{R}^2 plane in order to visualize the deficit angle ϵ_h . (b) The link hj is flipped to other link ik in such a way that the length of the link ik is the Euclidean distance between the vertices i and k .*

Fig. 10 (a). A hybrid $(2, 2)$ move makes the link hj flip to other link ik in such a way that the vertices i and k are connected by a straight line on the Euclidean space \mathbf{R}^2 , as shown in Fig. 10 (b). Evidently,

the deficit angles $\epsilon_h, \epsilon_i, \epsilon_j, \epsilon_k$ around h, i, j, k are invariant, because the following relations hold:

$$\begin{aligned}\theta_h^{(1)} + \theta_h^{(2)} &= \tilde{\theta}_h^{(1)}, & \theta_i^{(1)} &= \tilde{\theta}_i^{(1)} + \tilde{\theta}_i^{(2)}, \\ \theta_j^{(1)} + \theta_j^{(2)} &= \tilde{\theta}_j^{(2)}, & \theta_k^{(1)} &= \tilde{\theta}_k^{(1)} + \tilde{\theta}_k^{(2)}.\end{aligned}\quad (15)$$

where $\theta_v^{(m)}$ and $\tilde{\theta}_v^{(m)}$ ($v = h, i, j, k$; $m = 1, 2$) are shown in Fig. 10 (a) and (b). The sum of areas of the triangles also is invariant:

$$V_{hij} + V_{hjk} = V_{hik} + V_{ijk} . \quad (16)$$

Here the volumes V_σ ($\sigma = hij, hjk, hik, ijk$) denote areas of the 2-simplices considered. These simple relations (15) and (16) ensure that the local geometry and the Regge action (4) are exactly invariant under the move of Fig. 10. Hence, we call this hybrid (2, 2) move an *invariance (2, 2) move*. From a geometric viewpoint, the invariance (2, 2) move is a simplicial representation of a local coordinate transformation, because the 2-simplices hij, hjk, ijk themselves can be regarded as local coordinates and the move changes one local coordinate system spanned by hij and hjk to another spanned by hik and ijk . Furthermore, it keeps exactly invariant the local geometry in the simple way. Therefore, we can naturally interpret the invariance (2, 2) move as a lattice diffeomorphism in the sense of “invariance of the geometry”.

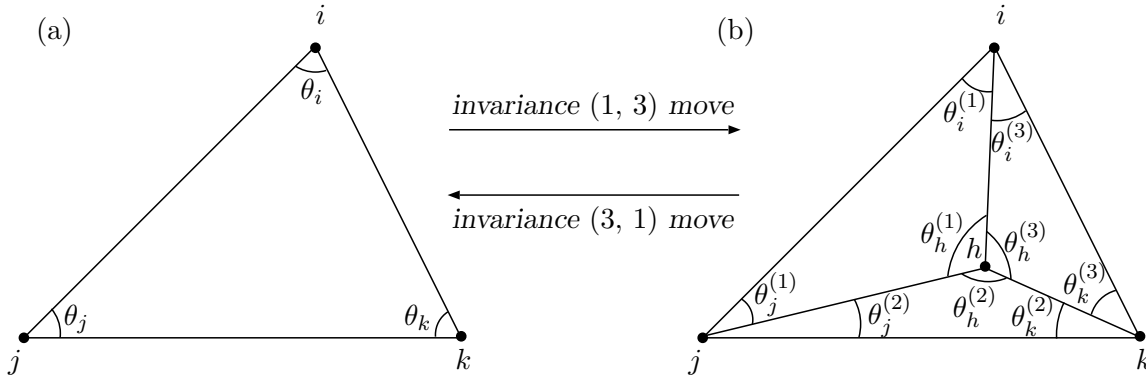


Figure 11: Example of the invariance (1, 3) move, which keeps invariant the simplicial geometry and the Regge action (4). (a) A triangle ijk is put on a flat \mathbf{R}^2 plane. (b) The triangle is subdivided into three triangles hij, hjk and hki in such a way that the length of the link hi is the Euclidean distance (straight line) between h and i and, in the similar way, the lengths of hj and hk are chosen to be the Euclidean distances.

In a similar way, we can define other invariance moves as shown in Fig. 11. We first pick up a 2-simplex ijk shown in Fig. 11 (a), and then subdivide it into three simplices hij, hjk and hki in Fig. 11 (b) by putting a new vertex h inside ijk and connecting it with i, j, k in such a way that the flatness property inside ijk is preserved. Under the action of this move, the invariance of the deficit angles $\epsilon_i, \epsilon_j, \epsilon_k$ around i, j, k is guaranteed simply by the following relations:

$$\theta_i = \theta_i^{(1)} + \theta_i^{(3)}, \quad \theta_j = \theta_j^{(1)} + \theta_j^{(2)}, \quad \theta_k = \theta_k^{(2)} + \theta_k^{(3)} . \quad (17)$$

Here, the dihedral angles θ_v and $\theta_v^{(m)}$ ($v = i, j, k$; $m = 1, 2, 3$) are shown in Fig. 11 (a) and (b). The deficit angle ϵ_h around the inserted vertex h is exactly zero, because the Euclidean flat geometry inside the triangle ijk is preserved exactly, namely, the following equality holds:

$$2\pi = \theta_h^{(1)} + \theta_h^{(2)} + \theta_h^{(3)}. \quad (18)$$

The total volume also is invariant under the move:

$$V_{ijk} = V_{hij} + V_{hjk} + V_{hki}, \quad (19)$$

where the volumes V_σ denote areas of the 2-simplices $\sigma = ijk, hij, hjk$ and hki in Fig. 11. We call this hybrid (1, 3) move an *invariance (1, 3) move*, and its inverse an *invariance (3, 1) move*. These relations (17), (18) and (19) guarantees the exact invariance of the local geometry under the invariance moves. These moves can be interpreted as the lattice diffeomorphisms in the same way as the invariance (2, 2) move could be.

It is straightforward to generalize the two-dimensional invariance (p, q) moves to higher-dimensional ones, which keep exactly invariant both the local geometry and the Regge action in the similar way. For example, we consider the three-dimensional case. Let us remember Fig. 7, where the 3-simplex $v_0v_1v_2v_3$ is divided into the four 3-simplices by the hybrid (1, 4) move. If one adjusts the lengths l_0, l_1, l_2, l_3 so that the geometry inside $v_0v_1v_2v_3$ remains flat, the deficit angles around the six links of $v_0v_1v_2v_3$ are invariant, and furthermore, deficit angles around the four inserted links are zero (flat) in Fig. 7 (b). The sum of volumes of the four new 3-simplices is exactly equal to that of $v_0v_1v_2v_3$. This is an invariance (1, 4) move that keeps the Regge action (4) invariant in three dimensions. Similarly, one can construct an invariance (2, 3) and an invariance (3, 2) moves.

In addition to the symmetry described above, the permutation group, S_{N_0} , of N_0 vertices gives another invariance, corresponding to re-labeling of vertices on the lattice. Therefore, we conclude that *the lattice diffeomorphisms in the sense of invariance of the geometry are generated by both the invariance (p, q) moves and the permutation group S_{N_0} in DRC*. Symbolically, we denote the symmetry of DRC as follows:

$$\{\text{lattice diffeomorphisms}\} = \{\text{moves generated by invariance } (p, q) \text{ moves}\} \ltimes \bigoplus_{N_0=1}^{\infty} S_{N_0}. \quad (20)$$

What does this symmetry imply to lattice quantum gravity? One might naively hope that one can simply integrate over the gauge transformations (the lattice diffeomorphisms) without any gauge-fixing procedure just as one can in lattice gauge theories. However, this is *not* the case with gravitation [11]; the crucial difference between Einstein's gravity and gauge theories is that the symmetry group is *non-compact* in theories of (lattice) gravity. Thereby, one must factor out the *infinite* volume of the diffeomorphism group to make sense of the path integral for the gravitational field. Thus, it is plausible that the infinite volume of the lattice diffeomorphisms would prevent the entropy bound (12) from holding. However, it is very difficult to prove (or deny) the inequality (12) by analytic methods, because the entropy (9) depends on the triangle inequalities which are too complicated to estimate analytically. Moreover, it will also depend on the measure chosen for the link-integration. Hitherto,

we deform the problem to another one: what measure enables the exponential bound (12) to hold? In section 5, we will investigate numerically the (un)boundedness of the entropy (9) using two types of measures.

4.2 Black hole entropy in DRC

Before turning to numerical studies, let us now apply the lattice symmetry to the black hole entropy¹⁰ problem. Among various attempts to solve the problem, Carlip advocated that by virtue of the horizon structure, the “would-be gauge freedom” of general covariance supplies physical states of the Kerr black holes in arbitrary dimensions [55]. In spite of some shortcomings in his analysis [56], his idea has attracted much attention to the relation between the entropy and the horizontal geometry of black holes. Indeed, it is argued in ref. [57] that the diffeomorphism on the event horizon can be regarded as a nontrivial asymptotic isometry of the Schwarzschild black hole. In what follows, we discuss a simple method of deriving the black hole entropy from a lattice-theoretic viewpoint; the derivation is based on the lattice diffeomorphisms (20) in DRC.

Suppose that there exists a simplicial lattice that corresponds to a four-dimensional black hole with a triangulated horizon S^2 of area A . We define G_{HM} as a set of all the moves generated by the hybrid (p, q) moves acting on the triangulated black hole. We define also a subset $H_{\text{HM}} \subset G_{\text{HM}}$ as

$$H_{\text{HM}} \equiv \left\{ f \in G_{\text{HM}} ; f \notin \{\text{lattice diffeomorphisms}\}, f|_{S^2} \neq \text{identity, and} \right. \\ \left. f|_{S^2} \in \{\text{lattice diffeomorphisms on the triangulated horizon } S^2 \} \right\}. \quad (21)$$

An example of an element $f \in H_{\text{HM}}$ is depicted on Fig. 12. Physically, each element $f \in H_{\text{HM}}$ means such a quantum fluctuation that is a nontrivial combination of the hybrid (p, q) moves acting on the triangulated horizon; its restriction, $f|_{S^2}$, on the horizon is required to be a two-dimensional lattice diffeomorphism on the horizon to keep invariant the horizontal geometry.

Assuming that there exist n_{P} elements of H_{HM} per the Planck area $\ell_{\text{P}}^2 = G\hbar/c^3$, we can easily count the total number of such fluctuations, N_{fluc} , around the horizon in a combinatorial way:

$$N_{\text{fluc}} \sim (n_{\text{P}})^{A/\ell_{\text{P}}^2}.$$

This number N_{fluc} corresponds to the total number of quantum fluctuations that keep invariant the simplicial geometry on the horizon; thereby one can define an entropy \mathcal{S}_{BH} of the black hole as

$$\mathcal{S}_{\text{BH}} \equiv k_{\text{B}} \log N_{\text{fluc}} \sim k_{\text{B}} \log n_{\text{P}} \cdot \frac{A}{\ell_{\text{P}}^2}. \quad (22)$$

Here, our idea of the derivation of the black hole entropy is based on the simple picture that any quantum states are associated with quantum fluctuations; the classical picture of the horizon should accompany many fluctuations around it at a quantum level, and the huge entropy of the black hole arises from the contribution of such fluctuations.

¹⁰Here I make a simple remark. The Bekenstein-Hawking black hole entropy (1) has nothing to do with the entropy bound (12). Don’t be confused by the same terminology ‘entropy’.

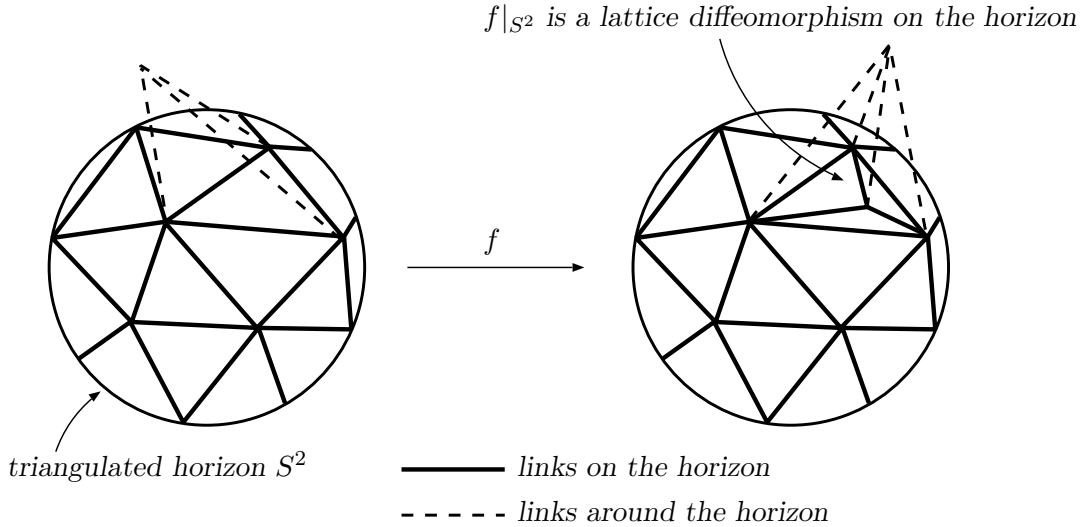


Figure 12: Example of a combination of the hybrid moves $f \in H_{HM}$ defined by eq. (21). On the triangulated horizon S^2 , $f|_{S^2}$ is required to be a two-dimensional lattice diffeomorphism.

However, we encounter a difficult problem: If one takes a continuum limit, the fluctuation density n_P will diverge, resulting in an infinite value of the entropy \mathcal{S}_{BH} in eq. (22). Such a divergent behavior of the black hole entropy often appears also in continuum approaches. In particular, Susskind and Uglum [21] showed that the entropy per unit area of a free scalar field propagating in a fixed black hole background is quadratically divergent near the horizon and such quantum corrections to the black hole entropy area are equivalent to quantum corrections to the gravitational coupling constant G , although the theory of interest is non-renormalizable. They argued that the question on the finiteness of the entropy is inextricably intertwined with the renormalization of the coupling G and, therefore, concluded that the finiteness property cannot be understood without the complete knowledge of the ultra-violet behavior of the theory.

Taking the discussions in the continuum into consideration, we are led to the following idea: If we regard the lattice model (8) as an effective theory with a finite cutoff l_{\min}^{-1} , the fluctuation density n_P will remain finite in eq. (22). This finiteness enables us to avoid the divergence behavior and, furthermore, to normalize the Planck length ℓ_P in eq. (22) so as to set

$$n_P = e^{1/4} (= 1.284 \dots) . \quad (23)$$

As a consequence, we reach the following expression:

$$\mathcal{S}_{BH} \sim \frac{k_B}{4} \frac{A}{\ell_P^2} . \quad (24)$$

Thus, eq. (24) agrees with the Bekenstein-Hawking area law of the black hole entropy (1).

How can we interpret the relations (23) and (24) on physical ground? Interestingly enough, the notion of the *space-time uncertainty principle* has been advocated in the development of string theory and noncommutative field theory [49]. According to the principle, space-time has an uncertain property

in itself; uncertainty of temporal coordinate ΔT and that of spatial one ΔX satisfy

$$\Delta T \Delta X \geq \ell_s^2 , \quad (25)$$

where ℓ_s is the so-called string scale of order $O(\ell_P)$. Here the lengths ΔT and ΔX are defined in a conformally invariant way, called the extremal length. A natural interpretation of the relation (25) is given in the context of noncommutative geometry [50], in which the coordinates are promoted to operators that satisfy commutation relations similar to those of quantum mechanics. However, we take another interpretation of the uncertainty principle (25); space-time has the intrinsic minimal length¹¹ ℓ_s and we identify it with the UV cutoff l_{\min} of DRC:

$$\Delta T_{\min} = \Delta X_{\min} = \ell_s \sim l_{\min} . \quad (26)$$

As a result, the uncertainty principle can be satisfied without introducing noncommutativity of space-time. According to this interpretation, eq. (23) means that on the minimal area $l_{\min}^2 \sim \ell_P^2$, we observe about one quantum fluctuation of the (lattice) gravitational field.

5 Numerical study of 3D pure gravity

In this section we turn to numerical studies in order to explore non-perturbatively the ground state of DRC (8) and the behavior of the entropy (9). We will calculate some observables (integrated curvatures, average link-length, and surface area distribution functions characterizing a fractal structure of space-time) for studying three-dimensional pure gravity by the Monte-Carlo method.

First, we rewrite the integration measure $d\mu_T[l]$ in the following form convenient for our numerical studies:

$$\int d\mu_T[l] = \prod_{i=1}^{N_1} \int_{l_{\min}}^{l_{\max}} dl_i \exp\left(-\tilde{S}[l, T]\right) \delta_T(\Delta) , \quad (27)$$

where $\delta_T(\Delta)$ stands for the constraints by the (higher-dimensional analogs of) triangle inequalities, and we denote the measure-induced part of the action as $e^{-\tilde{S}[l, T]}$. A few examples of the measure-induced part $\tilde{S}[l, T]$ will soon appear. From now on we set the minimum lattice spacing l_{\min} to be 1¹².

In the DT approach, the number of d -simplices, N_d , fluctuates largely in higher dimensions ($d = 3, 4$), making statistics of numerical data fairly worse. Similarly, such fluctuations occur also in our hybrid model. In order to obtain better statistics of our numerical data, we add an extra term $(N_d - V)^2$ to the Regge action (4); it controls the volume fluctuations around the designed size V . Hence, the total action, $S[l, T]$, on the lattice becomes of the form:

$$S[l, T] = S_{\text{Regge}}[l, T] + \tilde{S}[l, T] + \gamma(N_d - V)^2 . \quad (28)$$

¹¹Actually, it is discussed in ref. [51] that a particular uncertainty relation leads to the minimal length for each component of the space-time coordinates, namely, eq. (26) may be satisfied also in string theory.

¹²If dimensional arguments are needed, the appropriate power of the lattice spacing (which has the dimension of length) can always be restored at the end of calculations by invoking dimensional arguments.

Here γ is a small constant. As a result, the partition function of our hybrid model is defined as

$$Z_{\text{DRC}} = \sum_{T:\text{triangulations}} \int \prod_i dl_i \exp(-S[l, T]) \delta_T(\Delta) , \quad (29)$$

where the sum $\sum_{T:\text{triangulations}}$ admits only simplicial manifolds satisfying the manifold condition. Numerically, the sum of lattice configurations appearing in (29) is carried out through the hybrid (p, q) moves, as explained in section 3.2 (see Fig. 7).

From now on we focus on three-dimensional pure gravity. The topology of the simplicial lattice is fixed to three-sphere S^3 ; this is due to statistical and algorithmic difficulties in simulating manifolds with various topologies. In other words, we never consider the topology-changing process in our numerical study, and the numerical realization of such processes is a future challenging problem.

5.1 Phase structure of 3D pure gravity

In general, local operators cannot be gauge-invariant observables in quantum gravity. But some global quantities are gauge-invariant, for example, the average scalar curvature per volume:

$$\langle R \rangle \equiv \left\langle \frac{\sum_i l_i \epsilon_i}{\sum_\sigma V_\sigma} \right\rangle . \quad (30)$$

Here ϵ_i is the deficit angle around the i -th link (hinge) l_i and V_σ being the volume of a 3-simplices σ . This quantity $\langle R \rangle$ plays the role of the order parameters. The average length of all the links is also a good observable:

$$\langle l \rangle \equiv \left\langle \frac{\sum_i l_i}{N_1} \right\rangle . \quad (31)$$

These observables (30) and (31) can be calculated by the standard Monte-Carlo technique. In what follows, we perform numerical simulations using two types of measures, that is, the uniform measure $\prod_i dl_i$ and the scale-invariant one $\prod_i dl_i/l_i$. The number of 3-simplices N_3 is almost fixed at around a size $V = 5000$, and each link-length l_i is integrated over an interval $1 < l_i < 10$. The coefficient of the extra term to make small the fluctuation of N_3 is set at a value $\gamma = 1.0 \times 10^{-5}$. We will also measure a fractal structure based on a geodesic distance.

5.1.1 Calculation using the uniform measure

Here we adopt the uniform measure in simulating DRC (8):

$$d\mu_T[l] = \prod_{i=1}^{N_1} dl_i \delta_T(\Delta) . \quad (32)$$

In this case, the lattice action $S[l, T]$ is of the following simple form:

$$S[l, T] = S_{\text{Regge}}[l, T] + \gamma(N_3 - V)^2 . \quad (33)$$

The partition function becomes

$$Z_{\text{DRC}}^{\text{uniform}} = \sum_T \int \prod_i dl_i \exp(-S[l, T]) \delta_T(\Delta) . \quad (34)$$

However, the measure (32) causes a severe problem that the hybrid system (34) will not be well-defined statistical-mechanically. This is due to the reason that the entropy bound (12) for the configuration entropy (9) will not hold in this case. Now we must discuss this point in more detail.

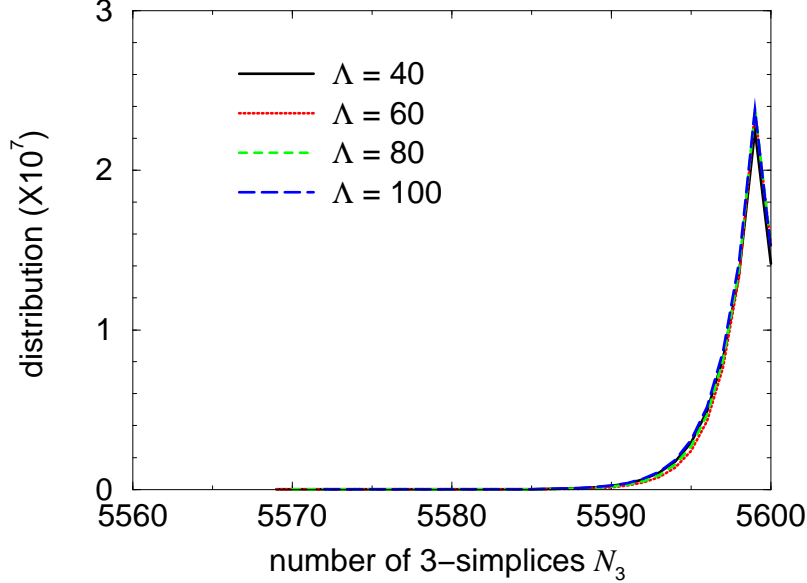


Figure 13: The N_3 distribution using the uniform measure $\prod_i dl_i$. The coupling constant G is set to be ∞ . Different curves correspond to different values of the cosmological constant ranging from $\Lambda = 40$ to $\Lambda = 100$. The maximum value of the horizontal axis is the upper cutoff of N_3 .

Actually, we tried carrying out numerical calculations using the measure (32). In our numerical data with $G = \infty$ (strong coupling limit), however, the number of 3-simplices N_3 exhibits a clear tendency to diverge, even though we set large values of the cosmological constant Λ , as shown in Fig. 13. Though the value of the cosmological constant varies from 40 to 100 in Fig. 13, the N_3 distribution is squeezed to the upper cutoff $N_3 = 5600$. Even if we choose larger values of the cutoff, the divergence behavior still appears in the same way. Hence, we cannot control the system (34) at all. From a viewpoint of statistical mechanics, one can interpret such a pathological behavior of the N_3 distribution as follows. If the entropy bound (12) does not hold, the configuration entropy $W(N_3)$ (see eq. (9)) will dominate the system in the strong-coupling phase (high-temperature phase). In other words, lattice configurations with large N_3 will frequently appear owing to the large values of the entropy $W(N_3)$. Actually, this is the case with our calculation using the uniform measure in Fig. 13. The large volume of the lattice diffeomorphisms would make large (presumably infinite) the entropy of such a pathological configuration. In that sense the data of Fig. 13 indicates a piece of numerical evidence for the existence of the lattice symmetry.

At any rate, our calculation using the uniform measure cannot proceed further and, therefore, we attempt to use other measure that breaks the diffeomorphism invariance at a quantum level.

5.1.2 Calculation using the scale-invariant measure

Next, we attempt to simulate the system (29) using the scale-invariant measure:

$$d\mu_T[l] = \prod_{i=1}^{N_1} \frac{dl_i}{l_i} \delta_T(\Delta) . \quad (35)$$

Obviously, this measure is invariant under local rescalings $l_i \rightarrow c_i l_i$ where c_i are constants. In this case, the partition function is defined as follows:

$$Z_{\text{DRC}}^{\text{scale-inv}} = \sum_T \int \prod_i dl_i \delta_T(\Delta) \exp(-S[l, T]) , \quad (36)$$

where the action $S[l, T]$ is of the form:

$$S[l, T] = S_{\text{Regge}}[l, T] + \sum_{i=1}^{N_1} \log l_i + \gamma(N_3 - V)^2 . \quad (37)$$

First of all, we measure the N_3 distribution, as shown in Fig. 14. One observes in the figure that N_3 distributes smoothly around the central value $V = 5000$, in contrast to the uniform-measure case shown in Fig. 13. According to the numerical data of Fig. 14, one can naively expect that the exponential bound (12) will hold under this measure.

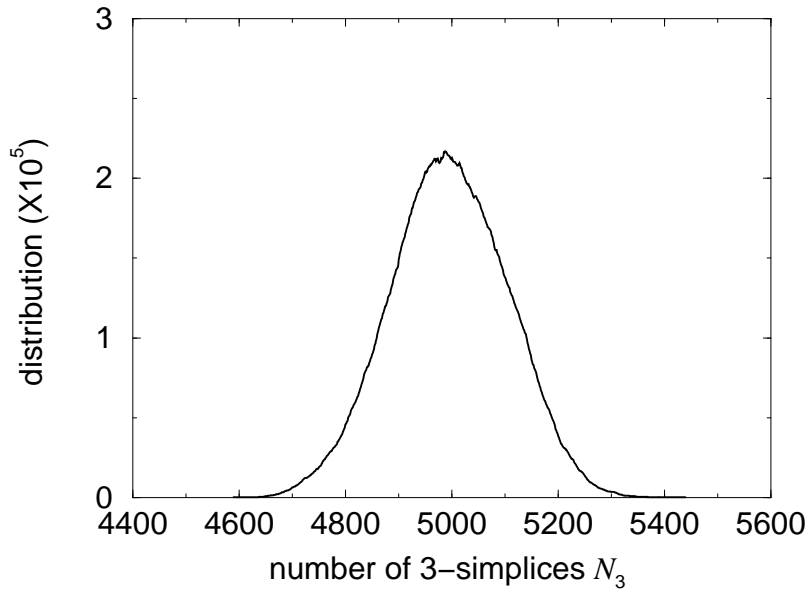


Figure 14: N_3 distribution using the scale-invariant measure $\prod_i dl_i/l_i$.

In this case, one can obtain in principle any observables numerically, unlike the case of the uniform measure. Indeed, we measured the integrated scalar curvature per volume, $\langle R \rangle$, as shown in Fig. 15. Evidently, this system has two phases, namely, the strong and the weak coupling phases; the solid line represents the cooling process from the strong coupling phase to the weak one, and the dotted its inverse. One can clearly observe a large hysteresis in Fig. 15, suggesting the first-order nature of the transition. It is consistent with results obtained in numerical studies of the three-dimensional DT model [43].

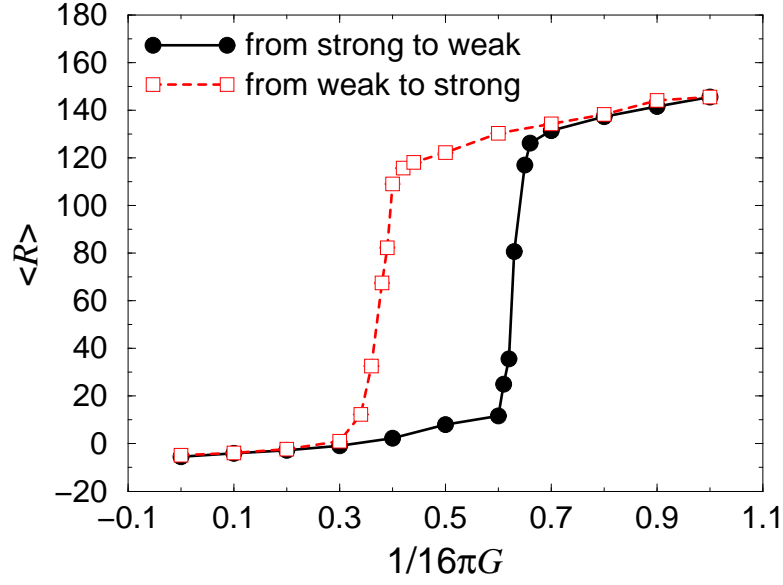


Figure 15: Hysteresis for the curvature $\langle R \rangle$ under the scale-invariant measure $\prod_i dl_i/l_i$. The solid line means the process from the strong to the weak coupling phase and the dashed vice versa.

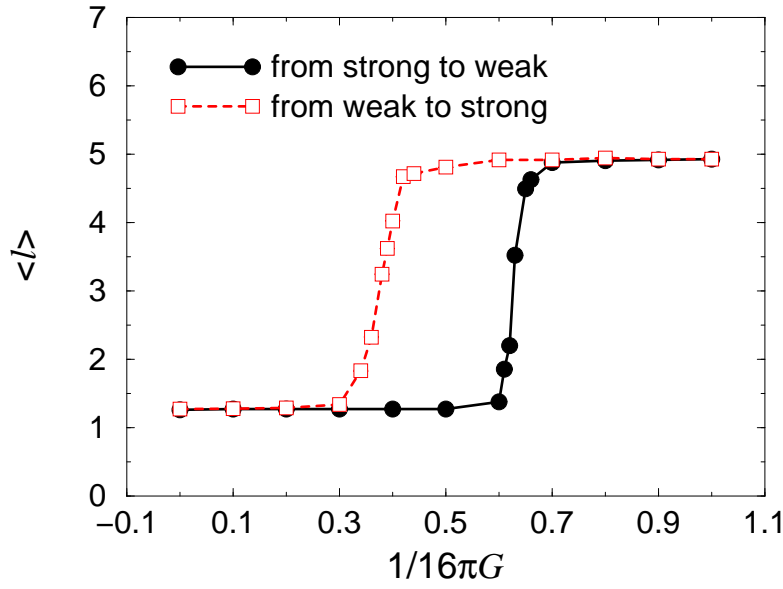


Figure 16: Hysteresis for the average link-length $\langle l \rangle$ under the scale-invariant measure $\prod_i dl_i/l_i$. The solid line means the process from the strong to the weak coupling phase and the dashed vice versa.

Next, we measured the average link-length $\langle l \rangle$ shown in Fig. 16, where we observe another large hysteresis. In the strong-coupling phase, the strong gravitation prevents spacetime manifolds from extending widely, resulting in the small value of the length $\langle l \rangle$. In the weak coupling phase, conversely, spacetime manifolds tend to stretch as widely as possible, resulting in spiky configurations. Such spikes of spacetime manifolds often appear also in the weak-coupling phase of quantum RC [13]. In this sense, our data of Fig. 16 is consistent with those obtained in the numerical studies of quantum RC.

Here we make a short remark on the statistics of our data. To get each point in Figs. 15 and 16, we accumulate 200 configurations, each of which is gained at an interval of 800 sweeps. Statistical errors are also included in the figures, although they are too small to be visible.

5.2 Fractal structure of 3D pure gravity

We can further investigate other structures of spacetime manifolds under the scale-invariant measure. Among them, a fractal structure based on a geodesic distance will be the most important, and its validity has been well established in two-dimensional DT [44]. Here we first explain the fractal structure and related issues for our purpose.

In the case of 3D gravity, the fractal structure is characterized by the *surface area distribution (SAD) function* $\rho(S, D)$ [45] and the *fractal dimension* d_f ; their definitions will be given right now and closely related to each other. The SAD function is defined as follows [45]: (i) Let us consider a connected graph \tilde{T} dual to a three-dimensional simplicial closed manifold T ; (ii) The *geodesic distance* between two points in \tilde{T} is defined as the minimum number of steps between the two points; (iii) We pick up a point P in the graph \tilde{T} (namely, a tetrahedron in T) and find all points that have a geodesic distance D from the starting point P ; (iv) The boundary manifold appearing in slicing T at the distance D consists of closed surfaces of various topologies, as shown in Fig. 17; (v) Then, the SAD function $\rho(S, D)$ is defined as

$$\rho(S, D) \equiv \text{the number of closed surfaces of area } S \text{ at a geodesic distance } D. \quad (38)$$

The fractal structure is encoded in the scaling behavior of the SAD function $\rho(S, D)$ with a scaling variable $x = S/D^\alpha$, where the exponent α has different values in different phases. $\rho(S, D) \times D^\alpha$ is expected to be a function only of x in scaling regions, and, therefore, it suggests a scaling law $S \sim D^\alpha$. Thus, a fractal dimension, d_f , of spacetime is determined as

$$d_f = \alpha + 1. \quad (39)$$

Intuitively, such a scaling means a self-similarity of ‘time slices’ that arise in cutting spacetime manifolds at different geodesic distances¹³.

Incidentally, the scaling behavior of $\rho(S, D)$ was observed numerically in three-dimensional DT [45], while its validity in studying quantum spacetime was first established in two-dimensional DT [44]. Moreover, a similar scaling behavior was reported also in four-dimensional DT [46].

¹³ Actually, one can think of the geodesic distance D as a temporal coordinate, corresponding to the so-called temporal gauge [47].

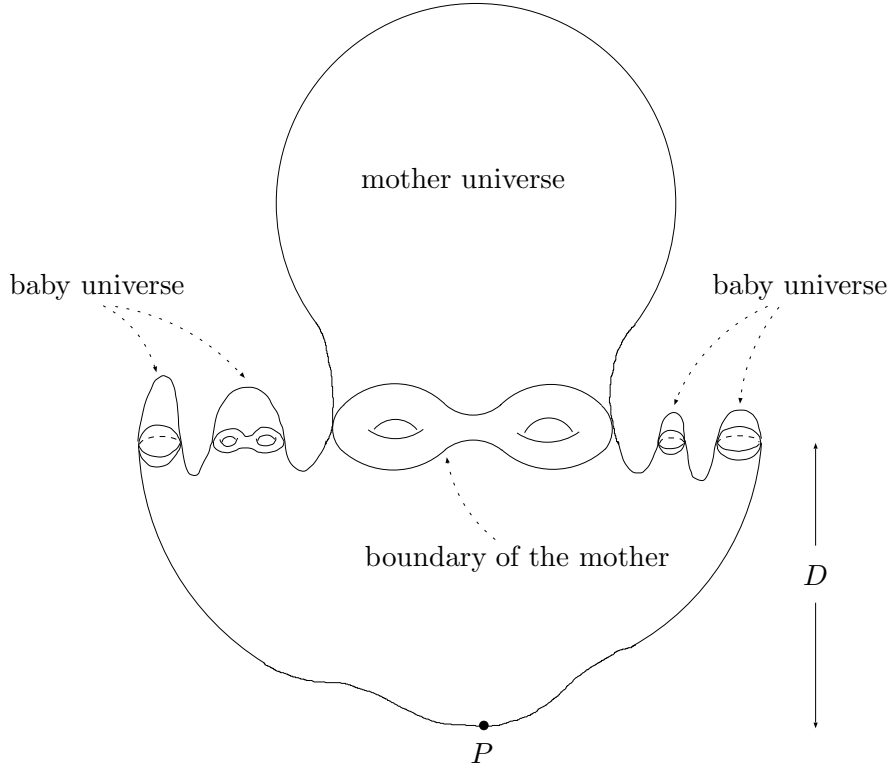


Figure 17: *Schematic picture of a three-dimensional fractal manifold that appears in the strong-coupling phase of DT. On the ‘time slice’ at a geodesic distance D one can find many closed surfaces as the boundary. The fractal structure is revealed as the scaling property of the distribution of the closed surfaces at various geodesic distances.*

According to the values of the gravitational constant G , we can classify the fractal structure into three regions: the strong-coupling region, the critical region, and the weak coupling region. An example of the fractal manifold with the scaling behavior is schematically depicted on Fig. 17, which occurs typically in the strong-coupling phase of three-dimensional DT. A closed surface of fairly large area appears only once at each ‘time slice’ D , which is the boundary of the so-called *mother universe*. Concurrently, there are many surfaces of small areas at each ‘time slice’ and they are boundaries of the *baby universes*. The boundaries of the mother and the baby universes consist of closed surfaces of various topologies.

Having reviewed the fractal structure of DT, we will devote our attention to the investigation of the similar structure of our hybrid model in the next section.

5.2.1 Fractal structure in the strong-coupling limit $G = \infty$

First, we measure the SAD function $\rho(S, D)$ in the strong-coupling limit $G = \infty$ in DRC. Numerical data obtained is shown in Fig. 18, where the vertical axis means the SAD scaling function of the form $\rho(S, D) \times D^{3.5}$ and the horizontal the scaling variable $x = S/D^{3.5}$. The different curves show several data measured at different geodesic distances $D = 5, 6, 7$ and 8. The boundary surface of the mother universe, which has the largest area among all boundaries, has a good scaling property with a scaling

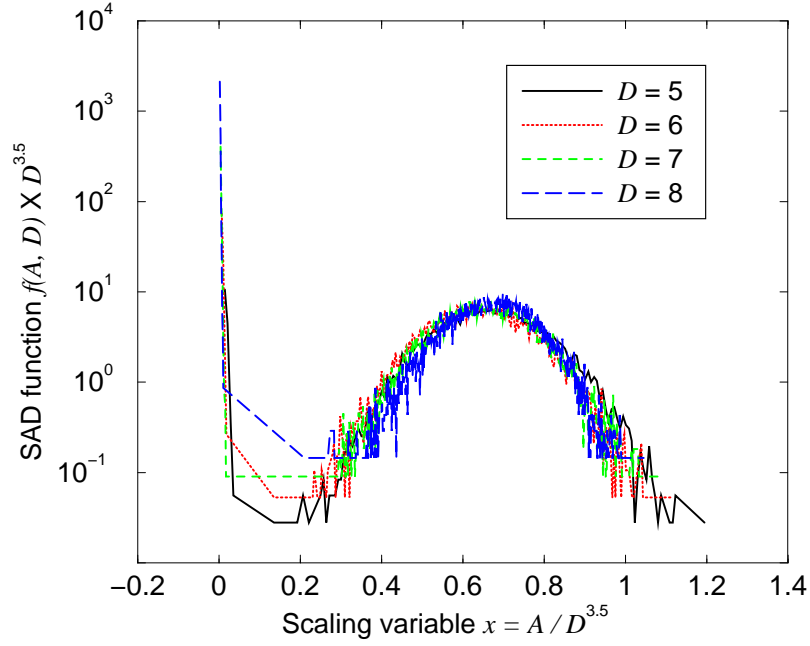


Figure 18: SAD function $\rho(S, D)$ in the strong-coupling limit $G = \infty$ in 3D pure gravity based on DRC. The number of 3-simplices are almost fixed at about $N_3 = 5000$ and each link-length l_i is integrated over a range $1 < l_i < 10$. The scale-invariant measure $\prod_i dl_i/l_i$ is used.

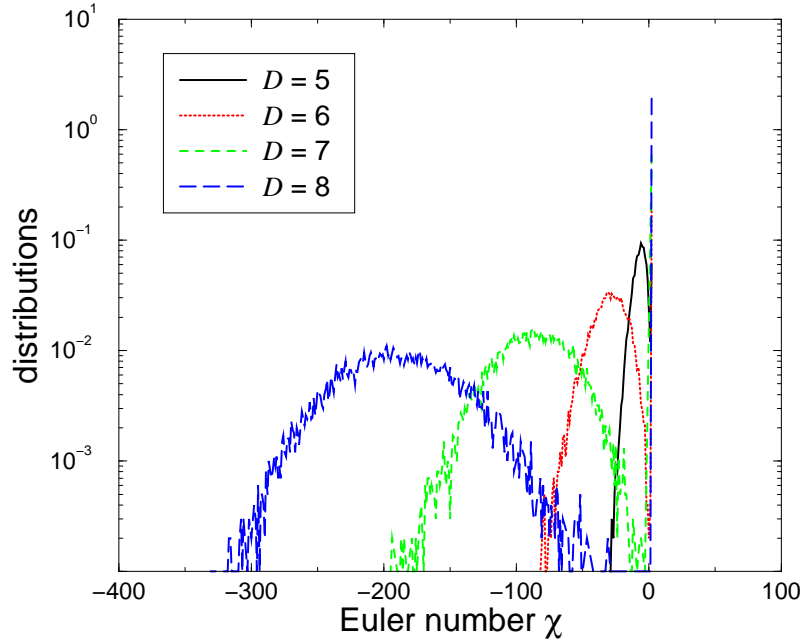


Figure 19: Distributions of the Euler number χ in the strong-coupling limit $G = \infty$ in 3D pure gravity based on DRC. Different curves corresponds to geodesic distances $D = 5, 6, 7$ and 8.

parameter $x = S/D^{3.5}$. Accordingly, the fractal dimension is obtained as $d_f = 3.5 + 1 = 4.5$. As observed clearly in Fig. 18, the distributions of the mother obey the Gaussian distribution. On the contrary, boundaries of the baby universes, whose areas are fairly smaller than that of the mother, do not exhibit a scaling behavior. In other words, it is impossible that the baby part scales in the same manner as the mother does; such an observation of two scaling variables in a manifold typically appear also in 3D DT [45].

Next, we measure the Euler number of the boundary surfaces. On each closed surface, the Euler number χ is defined in the usual way:

$$\chi \equiv n_0 - n_1 + n_2 \quad , \quad (40)$$

where n_k mean the numbers of k -simplices ($k = 0, 1, 2$) on each boundary surface. Our data of the Euler number χ are shown in Fig. 19; obviously, surfaces with large negative χ , exhibiting the complicated topologies, are identified with the boundary of the mother universe. The distributions of the mother are in the shape of mountain (Gaussian-like) and, in contrast, those of the baby universes have a sharp peak at $\chi = 2$. These results are consistent with those obtained in the strong-coupling phase of 3D DT [45].

How can we draw a physical picture of this region? One of plausible answers is a ‘confinement of spacetime’, into which all the volume of quantum spacetime is completely confined¹⁴. Actually, the large fractal dimension, whose value is $d_f \sim 3.5 + 1$ in this limit, will prevent spacetime from extending, although its volume is not small. In addition, the large negative values of χ frequently appear in the distributions of the mother; this complexity of the topology reminds us of the spacetime foam.

5.2.2 Fractal structure in the critical region $G \sim G_c$

Second, we measure the SAD function and the Euler number distribution at $1/16\pi G = 0.6$ in the critical region; the results are shown in Fig. 20 and Fig. 21, respectively. In Fig. 20, the vertical axis is the scaling function of the form $\rho(S, D) \times D^{2.3}$ and the horizontal one is the scaling variable $x = S/D^{2.3}$; the exponent 2.3 is very small compared with the value obtained in the strong-coupling limit. Thus, we obtain a smaller fractal dimension $d_f = 2.3 + 1 = 3.3$ in this region. In general, the smaller the fractal dimension becomes, the more widely the spacetime manifold extends.

In this region, one cannot separate the contribution of the mother from that of the baby universes, because the scaling function $\rho(S, D)$ distributes smoothly from small x to large one. We have learned in two-dimensional DT that the distribution of the mother boundary is universal and, hence, it has the close connection with the continuum limit [44]. On the other hand, the distribution of the baby boundaries is non-universal; interestingly, the result shown in Fig. 20 is very similar to that obtained in two-dimensional DT [44], although the first-order nature of the transition indicates no continuum limit in our case.

Next, we measure the χ distributions of closed surfaces that appear in cutting the simplicial space at each geodesic distance. The data is shown in Fig. 21, where the Euler number χ is measured at

¹⁴If one can obtain the ‘confinement’ picture also in four dimensions, it may be regarded as the confinement of gravitons. However, we are now in three dimensions, where no gravitons exist.

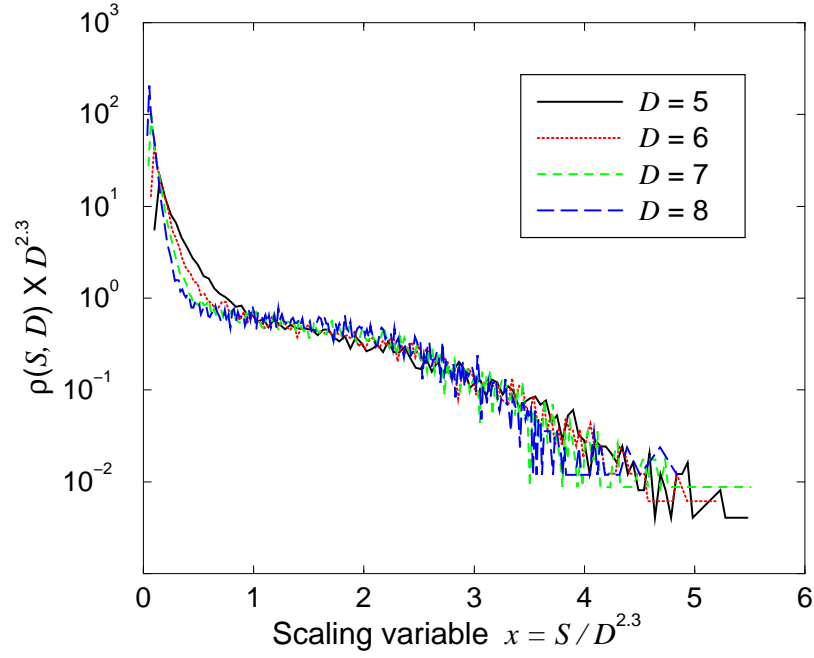


Figure 20: SAD function $\rho(S, D)$ near a critical point at $1/16\pi G = 0.6$ in 3D pure gravity based on DRC. The number of 3-simplices are almost fixed at about $N_3 = 5000$ and each link-length l_i is integrated over a range $1 < l_i < 10$. Scale-invariant measure $\prod_i dl_i/l_i$ is used.

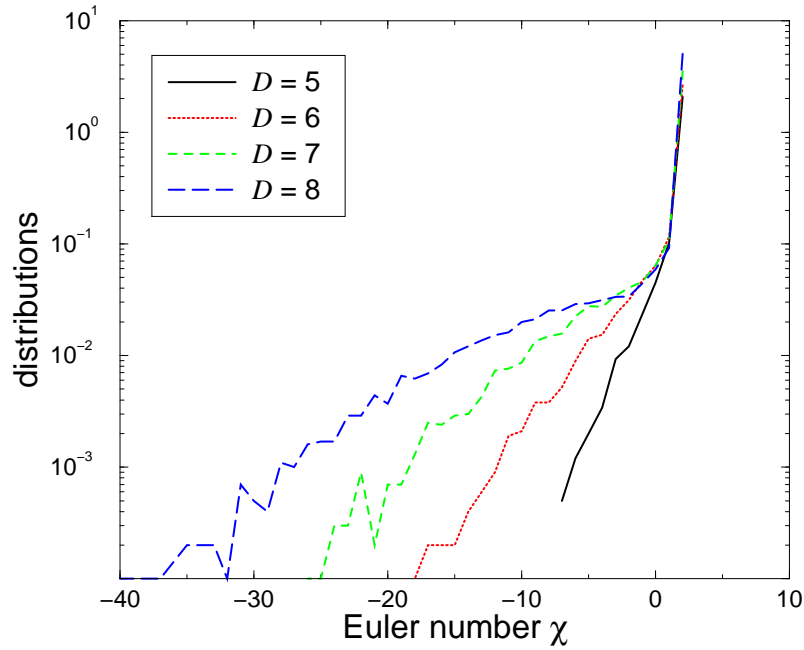


Figure 21: Distributions of the Euler number χ at $1/4\pi G = 0.6$ in the critical region of 3D pure gravity based on DRC. Different curves corresponds to different geodesic distances $D = 5, 6, 7$ and 8.

several distances. One sees that the χ distributions are fairly smoother than those of Fig. 19. As a result, we get a milder picture of spacetime in this region and, again, the shape of the χ distribution is very similar to those obtained in three-dimensional DT [45].

5.2.3 Fractal structure in the weak-coupling phase $G < G_c$

Lastly, in the weak-coupling phase, we attempted to measure the same quantity $\rho(S, D)$ in the same manner as in the strong-coupling and critical regions. However, we cannot find any contributions from a mother universe in this case and, what is worse, lattice configurations seemed to be almost frozen one with a lower fractal dimension; it strongly suggest the spiky nature of spacetime in this phase, and such a spike is far from the usual notion of physical spacetime. As is well known in numerical studies of DT, this phase corresponds to an elongated branched polymer with the small fractal dimension (for example, $d_f = 2$) [45]. Similarly, such spikes have been observed also in Monte-Carlo studies of quantum RC.

6 Conclusions and discussion

We have proposed dynamical Regge calculus (DRC) as a hybrid model of simplicial quantum gravity. This model is intended to make physical degrees of freedom larger than those of quantum Regge calculus (RC) and dynamical triangulations (DT). Furthermore, the extended model of DRC gives the possibility of describing the topology-changing processes of Euclidean spacetime in a dynamical way.

Algorithmically, the path integral for DRC (8) can be performed through the hybrid (p, q) moves, which are an extension of the ergodic (p, q) moves of DT. In particular, the lattice diffeomorphisms are generated by the invariance (p, q) moves. It is also an interesting problem that other constructive approaches to quantum gravity reproduce the same structure of the lattice diffeomorphisms as that of DRC, if one would believe the universality also in quantum gravity.

As an application of the lattice diffeomorphism, we attempted a lattice-theoretic derivation of the black hole entropy. We identified the total number of quantum fluctuations around the event horizon with the black hole entropy; such hybrid moves that keep invariant the horizontal geometry play the important role. In order to avoid the divergence of the coefficient of the entropy, we required the lattice cutoff l_{\min} to remain a finite value of order $O(\ell_P)$. The introduction of the minimal length seems to be consistent with a simple interpretation of the space-time uncertainty principle of string theory.

Moreover, we have carried out the numerical simulations of 3D pure gravity using the two kinds of the integration measures. In case of the uniform measure $\prod_i dl_i$ we observed the divergence behavior of the lattice size N_3 even though we chose the large values of the cosmological constant. This phenomenon indicates the exponential unboundedness of the entropy due to the lattice diffeomorphisms. In this case DRC is not well-defined statistical-mechanically. Therefore,

In case of the scale-invariant measure $\prod_i dl_i/l_i$, however, no pathological behavior occurred in our data. Indeed, we calculated the average curvature $\langle R \rangle$ and the average link-length $\langle l \rangle$; two pieces of

large hysteresis were observed, indicating the existence of the first-order transition between the two phases. In the strong-coupling phase, spacetime manifolds are crumpled to a singular configuration with a large fractal dimension. Physically, such a crumpled space might suggest the existence of ‘confinement’, into which spacetime itself is confined. In addition, various topologies appear on time slices of ‘confined spacetime’. In the critical region, we have obtained the smooth form of the SAD function, resulting in a milder picture of spacetime than in the strong-coupling limit. In this case spacetime looks a fractal manifold of lower fractal dimension. On the other hand, in the weak coupling phase simplicial configurations become spiky, and this phenomenon is essentially the same as that has been observed in the weak-coupling phase of quantum RC. Taking into account these theoretical and numerical studies, we conclude that DRC can reproduce the numerical results consistent with those of both DT and quantum RC in each region.

Our hybrid model of lattice quantum gravity offers a practical way of studying quantum black hole physics and the topology-change of Euclidean spacetime on the lattice. Incidentally, the close relation between 3D quantum gravity and quantization of the membrane theory [58] is an interesting theme in connection with string theory, though such an attempt generally gives rise to an instability problem [59]. At any rate, our chief concern is to investigate numerically the properties of strong-coupling quantum gravity within the framework of (extended) DRC.

Acknowledgments

I am grateful to K. Hamada for his detailed comments and suggestions. I would like to thank G. Kang for his useful comments on quantum black holes. I also wish to thank T. Yukawa and S. Horata for many useful discussions. Finally, I want to acknowledge valuable discussions with many members of Theory Division of KEK.

References

- [1] S. W. Hawking and G. F. R. Ellis, *The large scale structure of space-time*, Cambridge University Press (1973).
- [2] As texts of string theory, see, J. Polchinski, *STRING THEORY I, II*, Cambridge University Press (1998); M. B. Green, J. H. Schwartz and E. Witten, *Superstring theory I, II*, Cambridge University Press (1987).
- [3] For a review of loop quantum gravity, see, C. Rovelli, “*Loop Quantum Gravity*”, gr-qc/971008 (1997).
- [4] For a review of simplicial quantum gravity, see, F. David, “*Simplicial Quantum Gravity and Random Lattices*”, SACLAY preprint T93/028 (1993).
- [5] H. Hagura, “*Dynamical Regge Calculus as Lattice Gravity*”, Nucl. Phys. **B** (Proc. Suppl.) **94** (2001) 704.

- [6] H. Hagura, “*Quantum geometry in dynamical Regge calculus*”, Nucl. Phys. **B** (Proc. Suppl.) **106** (2002) 974.
- [7] D. Weingarten, Nucl. Phys. **B210** (1982) 229.
- [8] F. David, Nucl. Phys. **B257**[**FS14**] (1985) 45.
V. A. Kazakov, Phys. Lett. **B150** (1985) 282.
J. Ambjørn, B. Durhuus and J. Fröhlich, Nucl. Phys. **B257**[**FS14**] (1985) 433;
Nucl. Phys. **B275**[**FS17**] (1986) 161.
- [9] For the basic theory of quantum Regge calculus, see, H. W. Hamber, in *Critical Phenomena, Random Systems, Gauge Theories*, Proceedings of the Les Houches Summer School 1984, eds. K. Osterwalder and R. Stora, North-Holland (1986).
- [10] H. W. Hamber and R. M. Williams, Nucl. Phys. **B248** (1984) 392; **B269** (1986) 712.
- [11] M. Roček and R. M. Williams, Z. Phys. **C21** (1984) 371.
- [12] H. W. Hamber and R. M. Williams, Nucl. Phys. **B487** (1997) 345.
- [13] H. W. Hamber and R. M. Williams, Phys. Rev. **D47** (1993) 510.
- [14] M. Roček and R. M. Williams, Phys. Lett. **104B** (1981) 31.
- [15] H. W. Hamber, Nucl. Phys. **B20** (Proc. Suppl.) (1991) 728; Nucl. Phys. **B400** (1993) 347.
H. W. Hamber and R. M. Williams, Nucl. Phys. **B435** (1995) 361.
- [16] J. Cheeger, W. Muller and R. Schrader, Commun. Math. Phys. **92** (1984) 405.
- [17] J. Bekenstein, Phys. Rev. **D7** (1973) 2333; **D9** (1974) 3292.
- [18] S. W. Hawking, Commun. Math. Phys. **43** (1975) 199; Phys. Rev. **D13** (1976) 191.
- [19] S. W. Hawking, *Nature (Physical Science)*, **248** (1974) 30.
- [20] J. Bekenstein, “*DO WE UNDERSTAND BLACK HOLE ENTROPY ?*”, gr-qc/9409015.
- [21] L. Susskind and J. Uglum, “*Black Hole Entropy in Canonical Quantum Gravity and Superstring Theory*”, Phys. Rev. **D50** (1994) 2700-2711, hep-th/9401070.
- [22] I. Moss, Phys. Rev. Lett. **69** (1992) 1852; M. Visser, Phys. Rev. **D48** (1993) 583. R. Kallosh, T. Ortin and A. Peet, Phys. Rev. **D47** (1993) 5400.
- [23] M. Srednicki, Phys. Rev. Lett. **71** (1993) 666.
- [24] S. W. Hawking, “*The path-integral approach to quantum gravity*” in *General Relativity: an Einstein Centenary Survey* (ed. S. W. Hawking and W. Israel) Cambridge University Press, Cambridge (1979).
- [25] J. Distler and H. Kawai, Nucl. Phys. **B321** (1989) 509.
V. G. Knizhnik, A. M. Polyakov and A. B. Zamolodchikov, Mod. Phys. Lett. **A3** (1988) 819.
F. David, Mod. Phys. Lett. **A3** (1988) 1651.
- [26] D. J. Gross and A. A. Migdal, Nucl. Phys. **B340** (1990) 333.
M. R. Douglas and S. H. Shenker, Nucl. Phys. **B335** (1990) 635.
F. David, Nucl. Phys. **B257**[**FS14**] (1985) 45.

- [27] B. De Witt, “*Quantum Theory of Gravity: I. The Canonical Theory*”, Phys. Rev. **160** (1967) 1113; “*Quantum Theory of Gravity: II. The Manifestly Covariant Theory*”, Phys. Rev. **162** (1967) 1195; “*Quantum Theory of Gravity: III. Applications of the Covariant Theory*”, Phys. Rev. **162** (1967) 1239.
- [28] G. W. Gibbons and S. W. Hawking, “*Action integrals and partition function in quantum gravity*”, Phys. Rev. **D15** (1977) 2752; G. W. Gibbons, S. W. Hawking and M. J. Perry, “*Path integrals and the indefiniteness of the gravitational action*”, Nucl. Phys. **B138** (1978) 141.
- [29] K. Hamada and F. Sugino, Nucl. Phys. **B553** (1999) 283;
K. Hamada, Prog. Theor. Phys. **103** (2000) 1237; **105** (2001) 673.
- [30] T. Regge, “*General relativity without coordinate*”, Nuovo Cimento **19** (1961) 558.
- [31] B. DeWitt, “*The space time approach to quantum field theory*”, in *Relativity, Groups and Topology II*, eds. K. Osterwalder and R. Stora, North-Holland (1984).
- [32] B. DeWitt, Phys. Rev. **160** (1967) 1113.
- [33] H. Römer and M. Zähringer, Class. Quant. Grav. **3** (1986) 897.
- [34] R. M. Williams, Nucl. Phys. [Proc. Suppl.] **57** (1997) 73, and references therein.
- [35] H. W. Hamber, Nucl. Phys. (Proc. Suppl.) **25A** (1992) 150, and references therein.
- [36] For a brief review for both of classical and Regge calculus, see, R. M. Williams and P. A. Tuckey, Class. Quant. Grav. **9** (1992) 1409, and references therein.
- [37] H. W. Hamber and R. M. Williams, Nucl. Phys. **B267** (1986) 482.
- [38] M. Gross and H. W. Hamber, Nucl. Phys. **B364** (1991) 703.
- [39] H. W. Hamber, Int. J. Sup. Appl. **5** (1991) 84; Phys. Rev. **D45** (1992) 507.
- [40] J. Alexander, Ann. Math. **31** (1930) 292.
M. Gross and S. Varsted, Nucl. Phys. **B378** (1992) 367.
- [41] U. Pachner, Europ. J. Phys. Combinatorics **12** (1991) 129.
- [42] S. Iso and H. Kawai, Int. J. Mod. Phys. **A15** (2000) 651, hep-th/9903217.
- [43] D. V. Boulatov and A. Krzywicki, Mod. Phys. Lett. **A6** No.32 (1991) 3005;
J. Ambjørn and S. Varsted, Nucl. Phys. **B377** (1992) 557.
- [44] H. Kawai, N. Kawamoto, T. Mogami and Y. Watabiki, Phys. Lett. **B306** (1993) 19.
- [45] H. Hagura, N. Tsuda and T. Yukawa, Phys. Lett. **B418**, (1998) 273, hep-lat/9512016;
H. S. Egawa and N. Tsuda, Nucl. Phys. B (Proc. Suppl.) **63** (1998) 739, hep-lat/9711001
- [46] H. S. Egawa, T. Hotta, T. Izubuchi, N. Tsuda and T. Yukawa, Prog. Theor. Phys. **97** (1997) 539, hep-lat/9611028; H. S. Egawa, N. Tsuda and T. Yukawa, Nucl. Phys. B (Proc. Suppl.) **63** (1998) 736, hep-lat/9709099.
- [47] M. Fukuma, N. Ishibashi, H. Kawai and M. Ninomiya, Nucl. Phys. **B427** (1994) 139, hep-th/9312175; M. Ikehara, N. Ishibashi, H. Kawai, T. Mogami, R. Nakayama and N. Sasakura, Phys. Rev. **D50** (1994) 7467, hep-th/9406207
- [48] M. Lehto, H. B. Nielsen and M. Ninomiya, Nucl. Phys. **B272** (1986) 213; **B272** (1986) 228.

- [49] T. Yoneya, “*String Theory and the Space-Time Uncertainty Principle*”, Prog. Theor. Phys. **103** (2001) 1081, hep-th/0004074.
- [50] T. Yoneya, “*Space-time uncertainty and noncommutativity in string theory*”, Int. J. Mod. Phys. **A16** (2001) 945 (Proceedings of the ‘Strings 2000’, Int. conf. Michigan Univ. 2000), hep-th/0010172.
- [51] R. Guida, K. Konishi and P. Provero, Mod. Phys. Lett. **A6** (1991) 1487 and references therein.
- [52] J. A. Wheeler, “*On the nature of Quantum Geometrodynamics*”, Annals of Physics **2** (1957) 604; “*Neutrinos, Gravitation and Geometry*”, in *Proceedings of the International School of Physics, “Enrico Fermi”, Course XI* (Zanichelli, Bologna) (1960); *Geometrodynamics* (Academic Press, New York) (1962).
- [53] S. W. Hawking, “*Spacetime foam*”, Nucl. Phys. **B144** (1978) 349.
- [54] T. Eguchi, P. B. Gilkey and A. J. Hanson, “*Gravitation, Gauge Theories and Differential Geometry*”, Phys. Rep. **66** No. 6 (1980) 213.
- [55] S. Carlip, Phys. Rev. Lett. **D51** (1995) 632.
- [56] Mu-In Park and Jeongwon Ho, Phys. Rev. Lett. **83** (1999) 5595.
- [57] M. Hotta, K. Sakai and T. Sakai, “*Diffeomorphism on horizon as an asymptotic isometry of Schwarzschild black hole*”, gr-qc/0011043, TU-606.
- [58] E. Bergshoeff, E. Sezgin and P. Townsend, Phys. Lett. **B189** (1987) 75; Annals Phys. **185** (1988) 330.
- [59] B. de Witt, M. Luscher and H. Nicolai, Nucl. Phys. **B320** (1989) 135.
B. de Witt, J. Hoppe and H. Nicolai, Nucl. Phys. **B306** (1988) 545.